USGS
science for a changing world

Geologic Map of Loudoun County, Virginia

By Scott Southworth, William C. Burton,
J. Stephen Schindler, and Albert J. Froelich

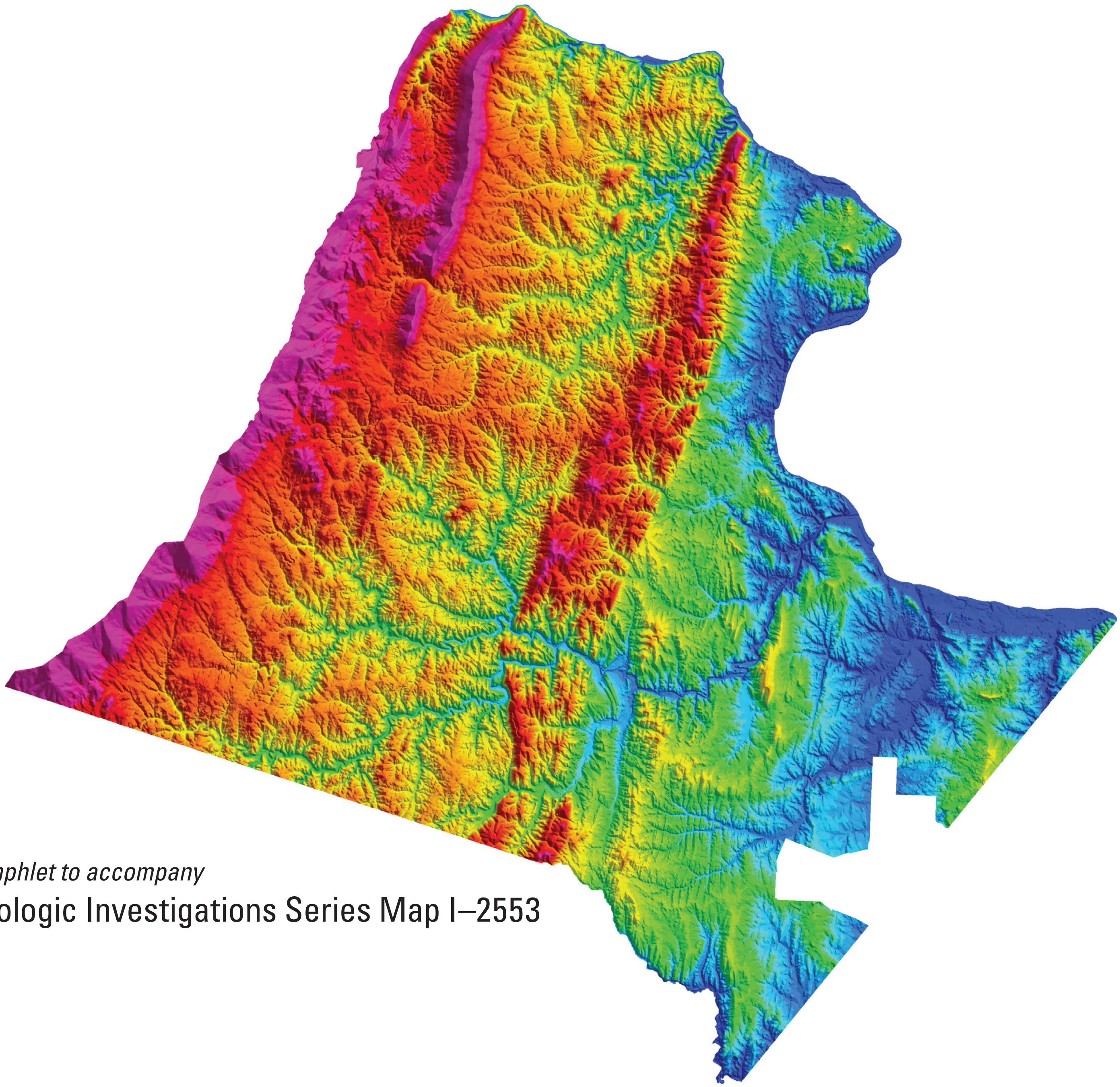

Pamphlet to accompany

Geologic Investigations Series Map I–2553

2006

U.S. Department of the Interior
U.S. Geological Survey

U.S. Department of the Interior
Dirk Kempthorne, Secretary

U.S. Geological Survey
P. Patrick Leahy, Acting Director

U.S. Geological Survey, Reston, Virginia: 2006
Revised: 2007

Cover: Color-shaded-relief image of Loudoun County, Va. (except the Dulles Airport area), showing high topographic elevations in shades of red and low topographic elevations in shades of blue. The hillshade is illuminated from the east. The highest elevation is 1,920 ft above sea level on Blue Ridge at the southwestern part of the county, and the lowest elevation is 180 ft above sea level along the Potomac River at the easternmost part of the county. The higher elevation region of the Blue Ridge province, in contrast to the lower elevation region of the Piedmont province in the eastern half of the county, is a function of rock hardness and different erosion histories. Image produced by Kerry Langueux and David L. Daniels, USGS, using 5-ft-contour-interval topographic data from the Loudoun County Office of Mapping and Geographic Information, Leesburg, Va.

For product and ordering information:
World Wide Web: http://www.usgs.gov/pubprod
Telephone: 1-888-ASK-USGS

For more information on the USGS--the Federal source for science about the Earth, its natural and living resources, natural hazards, and the environment:
World Wide Web: http://www.usgs.gov
Telephone: 1-888-ASK-USGS

Suggested citation:
Southworth, Scott, Burton, W.C., Schindler, J.S., and Froelich, A.J., 2006, Geologic map of Loudoun County, Virginia: U.S. Geological Survey Geologic Investigations Series Map I–2553, scale 1:50,000.

ISBN 1-411-30968-5

Printed on recycled paper

Contents

Introduction........1
Geologic Setting........1
Acknowledgments........1
Blue Ridge Province........1
Mesoproterozoic Basement Rocks........1
Nongranitic Rocks........2
Granitic Gneiss and Metagranite........3
Eastern Blue Ridge Units........3
Western Blue Ridge Units........3
Mesoproterozoic Metamorphism and Deformation........5
Monazite U-Pb Ages from Mesoproterozoic Rocks........5
Summary of Mesoproterozoic Geologic Events........7
Late Proterozoic Granite........8
Late Proterozoic Dikes........8
Dike Composition........8
Dike Orientation and Density........8
Geochemical Relation of Metadiabase Dikes to Metabasalt of the Catoctin Formation........9
U-Pb Age of Rhyolite Dike........9
Late Proterozoic Metasedimentary and Metavolcanic Rocks........9
Fauquier Formation........9
Swift Run Formation........22
Catoctin Formation........22
Age of the Catoctin Formation........22
Paleozoic Rocks of the Blue Ridge Anticlinorium........22
Loudoun Formation........23
Weverton Formation........23
Harpers Formation........23
Antietam Quartzite........23
Carbonaceous Phyllite........24
Tomstown Formation........24
Frederick Limestone........24
Paleozoic Structure........24
F_1 Folds and S_1 Cleavage........24
F_2 Folds and S_2 Cleavage........24
Faults........25
Paleozoic Metamorphism........25
$^{40}Ar/^{39}Ar$ Dating of Metamorphic Fabric........25
Piedmont Province........26
Potomac Terrane........26

Mesozoic Rocks of the Lower Culpeper Group 26
Manassas Sandstone 26
Reston Member....26
Poolesville Member....26
Balls Bluff Siltstone 26
Leesburg Member 26
Fluvial and Deltaic Sandstone and Siltstone Member 26
Lacustrine Shale and Siltstone Member 27
Catharpin Creek Formation 27
Mesozoic Rocks of the Upper Culpeper Group 27
Mount Zion Church Basalt 27
Midland Formation....27
Hickory Grove Basalt....27
Turkey Run Formation....27
Sander Basalt....28
Thermally Metamorphosed Rocks....28
Diabase Dikes and Sheets 28
Mesozoic Structure....28
Folds....28
Faults....28
Cenozoic Surficial Deposits 29
Terraces....29
Lag Gravel 29
Colluvium....29
Alluvium....29
Aeromagnetic Survey....29
Introduction....29
Data Reduction....30
The Color-Shaded-Relief Map 30
Correlation of Aeromagnetic Anomalies with Geology....30
References Cited....30

Figures

[On map sheet]

1. Map showing general geologic provinces and prominent geologic features of the area of and surrounding Loudoun County, Va.
2. Ternary diagrams showing quartz-alkali feldspar-plagioclase and normative feldspar of representative samples of the granitoid rocks in Loudoun County, Va.
3. Graphed equal-area projections (Schmidt net) of structural data of rocks in Loudoun County, Va.
4. Geochemical diagrams of the three types of metadiabase dikes in comparison with metabasalt of the Catoctin Formation
5. Color-shaded-relief aeromagnetic image of the Lincoln and most of the Bluemont 7.5-min quadrangles showing general geologic contacts

Tables

1. Point-count modes of representative samples of some Mesoproterozoic lithologies in Loudoun County, Va......2
2. Major element geochemical analyses and calculated norms of Mesoproterozoic rocks. 4
3. Ages related to intrusion of igneous rocks. 6
4. Major and minor element geochemical analyses of Late Proterozoic metadiabase dikes......10
5. Major and minor element geochemical analyses of Late Proterozoic metabasalt of the Catoctin Formation......18

Conversion Factors

Multiply	By	To obtain
inch (in)	2.54	centimeter (cm)
foot (ft)	0.3048	meter (m)
mile (mi)	1.609	kilometer (km)

Geologic Map of Loudoun County, Virginia

By Scott Southworth, William C. Burton, J. Stephen Schindler, and Albert J. Froelich

Introduction

The geology of Loudoun County, Va., was mapped from 1988 through 1991 under a cooperative agreement between the U.S. Geological Survey (USGS) and the Loudoun County Office of Mapping and Geographic Information. This geologic map was compiled in 1993 from a series of detailed published and unpublished field investigations at scales of 1:12,000 and 1:24,000. Some of these same data were compiled as a digital geologic map at 1:100,000 scale (Burton and others, 1992a) and were the basis for a cost-benefit analysis of the societal value of geologic maps (Bernknopf and others, 1993).

Geologic Setting

Loudoun County is underlain by rocks of two major physiographic provinces (fig. 1, on map sheet), the Blue Ridge province to the west and the Piedmont province to the east. Mesoproterozoic to Early Cambrian rocks underlie the Blue Ridge province as part of the Blue Ridge anticlinorium, a large, allochthonous fold that probably formed during the Paleozoic Alleghanian orogeny. The Blue Ridge anticlinorium is cored by high-grade Mesoproterozoic paragneiss and granitic gneisses, deformed and metamorphosed during the Grenville orogeny. Unconformable upon the basement gneisses is a cover sequence of Late Proterozoic to Early Cambrian metasedimentary and metavolcanic rocks. Late Proterozoic granite and a swarm of Late Proterozoic metadiabase and lesser metarhyolite dikes intruded the basement gneisses during continental rifting of Laurentia (North America) that resulted in the opening of the Iapetus Ocean (Rankin, 1975). These rocks were deformed and metamorphosed to greenschist facies during the Paleozoic Alleghanian orogeny. Rocks of the Piedmont province are predominantly Triassic and Jurassic strata of the Mesozoic Culpeper basin that are in contact with the east limb of the Blue Ridge anticlinorium along a major normal fault (fig. 1). Late Proterozoic to Early Cambrian metasedimentary rocks of the Potomac terrane (Drake and Morgan, 1981; Horton and others, 1989), exposed in the extreme northeastern corner of the county, accreted to Laurentia in the Taconian orogeny along the Pleasant Grove fault. Sedimentary and igneous rocks of the Culpeper basin accumulated during Mesozoic continental rifting that resulted in the opening of the Atlantic Ocean. Therefore the rocks of Loudoun County record a sequential tectonic history of orogeny (Mesoproterozoic Grenvillian), continental rifting (Late Proterozoic Iapetan), the transition from rift to passive continental margin (Early Cambrian), orogenic accretion and deformation (Middle Ordovician Taconian and late Paleozoic Alleghanian), and continental rifting (Triassic and Jurassic) and reflects several Wilson Cycles of opening and closing ocean basins (Wilson, 1966).

Cenozoic deposits that overlie the bedrock include terraces, lag gravels, colluvium, and alluvium. Terrace deposits of the ancestral Potomac River overlie Triassic sedimentary rocks as much as 235 ft above the present-day Potomac. Isolated lag gravel deposits superficially resemble terrace deposits but actually result from in situ weathering of Triassic and Jurassic conglomerates. Colluvium of boulders and cobbles mantles the high ground of the county, and thick concentrations are found in hillslope depressions on Blue Ridge, Short Hill, and Catoctin Mountains (Jacobson and others, 1990). Alluvium underlies the flood plains of the Potomac River and its tributaries.

Acknowledgments

Reviews by Peter T. Lyttle and Thomas R. Armstrong improved this report. We thank the Loudoun County Office of Mapping and Geographic Information for providing 5-ft-contour-interval topographic maps at a scale of 1:12,000. Avery A. Drake, Jr., and Robert R. Weems contributed the geologic mapping of the Piedmont province rocks. David L. Daniels, William F. Hanna, and Robert E. Bracken processed and interpreted the aeromagnetic data used in the color-shaded-relief image on the map sheet. The map was digitized by Remo Nardini, Peter G. Chirico, and James E. Reddy. Special thanks are extended to the private landowners who kindly provided access to their property.

Blue Ridge Province

Mesoproterozoic Basement Rocks

The Mesoproterozoic rocks that compose the core of the Blue Ridge anticlinorium consist of weakly to strongly foliated gneisses that exhibit high-grade metamorphic textures.

The gneisses can be divided lithologically into two groups, granitic gneisses and nongranitic gneisses. Moderately to strongly foliated granitic gneiss and weakly to moderately foliated metagranite compose over 90 percent by volume of the Mesoproterozoic basement. The volumetrically minor nongranitic lithic types include quartzite and quartz tectonite (Yq), paragneiss (Yp), metanorite and metadiorite (Yn), and quartz-plagioclase gneiss (Yqp). Protoliths of the quartzite, paragneiss, and metanorite are considered to be pregranitic (Burton and Southworth, 1993). Pyroxene-bearing granite or charnockite (Yc) also is found. Point-count modes of representative samples of some Mesoproterozoic lithologies are shown in table 1, and major element chemical analyses and calculated norms of some of the basement units are shown in table 2. Representative samples of the granitoid rocks (granitic gneiss plus quartz-plagioclase gneiss, metanorite, and charnockite) are plotted on a modal QAP diagram (fig. 2*A*, on map sheet). The granitoid rocks in table 2 are plotted on an An-Ab-Or diagram (fig. 2*B*, on map sheet).

Nongranitic Rocks

The Mesoproterozoic rocks include several units of probable sedimentary and igneous origin. These units occur as elongate lenses and layers within the voluminous granitic gneisses and may represent remnants of the country rock that existed prior to granitic intrusion (Burton and Southworth, 1993). The most distinctive, yet very poorly exposed, of these rocks is a graphite-bearing, garnet-rich paragneiss (Yp, table 1). It is distinctively rusty weathering and contains a strong Mesoproterozoic gneissosity defined by alternating quartz-plagioclase- and garnet-biotite-rich zones. Graphite generally occurs as evenly disseminated flakes less than 0.5 inch (in) across. The amount of garnet is highly variable and can range up to 25 percent. The mineralogy of the rusty paragneiss suggests that its protolith was an impure sandstone or graywacke (Burton and Southworth, 1993). The high silica content of the two paragneiss samples (table 2, sample nos. BR–660 and P41) is consistent with a metasedimentary origin. This unit resembles the Border Gneiss of Hillhouse (1960) in the central Virginia Blue Ridge, which is also garnet- and graphite-bearing, as described by Sinha and Bartholomew (1984) and Herz and Force (1984). Graphite-bearing, garnet-rich paragneiss can best be seen in a silage trench east of Airmont (Southworth, 1994) and along Catoctin Creek (Burton and others, 1995).

Hornblende-orthopyroxene-plagioclase gneiss or metanorite (Yn, table 1) is a spotted, medium- to coarse-grained, massive to locally well-foliated rock, in which orthopyroxene is the dominant mafic mineral while brown hornblende is secondary. Subordinate phases of this rock (undifferentiated on the map) are hornblende-biotite gneiss and amphibolite. These mafic rocks may have originated as dikes, sills, or flows within the original sedimentary terrane (Burton and Southworth, 1993). Two geochemical analyses of metanorite (table 2, sample nos. BR–602A and BR–1388) indicate diabase to diorite composi-

Table 1. Point-count modes of representative samples of some Mesoproterozoic lithologies in Loudoun County, Va.

[In percent. tr, trace; —, no data]

Map symbol ➤	**Yp**	**Yn**	**Yqp**	**Yc**	**Ygt**	**Yg**	**Ybg**	**Yhm**
Sample no. ➤	**BR–595**	**BR–602A**	**BR–36**	**B10**	**340 cut**	**BR–11**	**BR–554**	**PM**
Quartz	30	—	24	5	28	35	33	15
Plagioclase	43	58	45	65	28	22	23	23
Microcline (perthite)	—	—	—	10	40	39	19	38
Biotite	1	—	14	—	—	3	14	—
Garnet	5	—	—	—	5	—	—	—
Graphite	3	—	—	—	—	—	—	—
Orthopyroxene	—	35	—	15	—	—	—	—
Hornblende	—	5	—	5	—	—	—	23
Ilmenite/sphene	—	1	2	—	—	tr	tr	—
Apatite	—	tr	tr	—	—	—	—	—
Chlorite[1]	15	—	—	—	—	—	—	—
Clinozoisite/epidote[2]	1	1	7	—	—	—	2	—
Muscovite[2]	1	—	8	—	—	1	8	—
Rutile/sphene	2	—	—	—	—	—	—	—
Total, in percent	101	100	100	100	101	100	99	99
Total counts	537	508	571	340	563	592	556	316

[1]Secondary after garnet.

[2]Secondary after plagioclase.

tions. Metanorite can be seen near Milltown (Burton and others, 1995) and northwest of Morrisonville (Southworth, 1995). North of Middleburg, the body of metanorite is a pluton that contains metaperidotite, metagabbro, and metapyroxenite (Kline and others, 1994).

Quartzite and quartz tectonite (Yq) are gray to white, massive and fine-grained, and contain rounded grains of quartz and zircon. The quartzite lacks primary sedimentary structures and Grenville foliation but has a locally developed cleavage. The tan- to gray-weathering quartz tectonite is strongly cleaved and has white augen of recrystallized quartz, gray to black seams of carbonaceous phyllonite, and mappable internal pods of garnet-graphite paragneiss (Yp). Despite the lack of primary structures in these rocks, their spatial association with paragneiss suggests a sedimentary origin. Quartz tectonite can be seen east of Willisville (Southworth, 1994).

Quartz-plagioclase gneiss (Yqp) is restricted to the northeastern portion of the core of Mesoproterozoic rocks as narrow lenses within leucocratic metagranite (Yg) and biotite granite gneiss (Ybg). It is a white- and gray-weathering felsic rock that ranges from massive to well-foliated and has varying amounts of biotite and little or no potassium feldspar. This unit also is found to the north in Maryland where it has a U-Pb age of about 1,077±4 million years ago (Ma) (table 3, sample no. 11); this age is similar to that of the surrounding Group 3 granitic gneisses (table 3, sample nos. 9 and 10) and may have been derived through partial melting of a basaltic (Barker and Arth, 1976) or dacitic (Puffer and Volkert, 1991) protolith. Quartz-plagioclase gneiss can be seen west of Taylorstown (Burton and others, 1995).

Granitic Gneiss and Metagranite

Nine types of granitic rock are mapped on the basis of appearance, mineralogy, crosscutting relations, and isotopic age (table 3). With one exception biotite is the dominant mafic mineral, and some are very leucocratic in places. All of the granitic rocks are peraluminous except for hornblende monzonite gneiss (Yhm). Different types predominate west (western Blue Ridge) and east (eastern Blue Ridge) of the Short Hill fault. The granitic gneisses are divided into three groups on the basis of isotopic age (table 3) (Aleinikoff and others, 1993; Burton and others, 1994) and are, from oldest to youngest: Group 1 (1,153–1,140 Ma), Group 2 (1,112–1,111 Ma), and Group 3 (1,077–1,055 Ma).

Eastern Blue Ridge Units

Six types of granitic rock are mapped east of the Short Hill fault. The Marshall Metagranite (Ym) (Jonas, 1928; Espenshade, 1986) is the most common and is one of the Group 2 granites (table 3, sample nos. 12 and 13). It is a pink-weathering, weakly to moderately foliated, medium-grained biotite granite gneiss; biotite content ranges from 10 to 15 percent. The Marshall Metagranite can be seen along Goose Creek south of Leithtown. Biotite granite gneiss (Ybg) also has been mapped north to the Potomac River but is distinguished from the Marshall Metagranite on the basis of isotopic age (table 3, sample no. 7). Leucocratic metagranite (Yg) and garnetiferous leucocratic metagranite (Ygt), both Group 3 gneisses (table 3, sample nos. 9 and 10), are white-, light-gray-, or cream-weathering, medium- to medium-fine-grained, and massive to moderately foliated. They are differentiated primarily on the presence or absence of almandine garnet (table 1). The leucocratic metagranite is well exposed along the bluffs of the Potomac River north of Taylorstown (Burton and others, 1995).

Pink leucocratic metagranite (Yml), a Group 3 gneiss (table 3, sample no. 8) whose texture ranges from massive to moderately foliated, has the same pink-weathering aspect and grain size of the Marshall Metagranite. In contrast to the Marshall Metagranite, however, its biotite content ranges from 0 to about 10 percent. The map pattern suggests a thick, sill-like body that was intruded between the Marshall Metagranite and gneisses of the western Blue Ridge and enclosed a body of coarse-grained metagranite (Ymc). Pink leucocratic metagranite can be seen along Goose Creek south of St. Louis.

Coarse-grained metagranite (Ymc) has a distinctive texture consisting of 0.4- to 0.8-in-long, densely packed, white or pink microcline porphyroblasts and lesser interstitial plagioclase and distinctive blue quartz. This rock is typically quite massive showing only a weak Mesoproterozoic foliation of crudely aligned feldspar porphyroblasts. Coarse-grained metagranite has yielded a U-Pb age (table 3, sample no. 14) that is older than those of the adjacent Marshall Metagranite and pink leucocratic metagranite. Coarse-grained metagranite can be seen near Philomont. Some of these rocks may be equivalent to the coarse-grained phase of the Marshall Metagranite as mapped to the south by Espenshade (1986).

Western Blue Ridge Units

Six types of granitic rock are mapped west of the Short Hill fault. Medium- to coarse-grained, massive to well-foliated quartz-hornblende-orthopyroxene-microcline-plagioclase rock or charnockite (Yc) is mapped primarily on the basis of float. It is distinctive in having a greenish-black fresh surface and a crusty, pitted, orange-yellow weathering rind 0.4 to 0.8 in thick. Massive charnockite is found as a pod-like body within well-foliated hornblende monzonite gneiss (Yhm), northwest of Hillsboro (Southworth, 1995) while to the south, near Route 7, well-foliated charnockite occurs as linear bodies within various granitic gneisses (Southworth, 1994). The charnockite may have formed by the recrystallization of a preexisting hornblende-bearing phase (for example, the granite protolith for the hornblende monzonite gneiss (Yhm) under dry metamorphic conditions).

Porphyroblastic metagranite (Ypg) weathers yellowish-brown and consists of ovoid porphyroblasts of microcline 0.4 to 1.2 in. in diameter in a matrix of finer grained plagioclase and blue quartz. Biotite is the dominant mafic mineral, and garnet is also locally common. Despite its coarse grain size this rock is typically well foliated (table 3, sample nos. 15 and 17). Porphyroblastic metagranite can be seen southeast of Round Top (Southworth, 1994).

Table 2. Major element geochemical analyses and calculated norms of Mesoproterozoic rocks.

[In percent. Sample locations with the prefix BR are found in Burton and others (1995), and sample locations with the prefixes P and HF, and the 340 cut sample are found in Southworth (1994, 1995) and Southworth and Brezinski (1996). Sample of porphyroblastic metagranite (Ypg), prefixed by J, courtesy of P.T. Lyttle (unpub. data); samples of pink leucocratic metagranite (Yml) and Marshall Metagranite (Ym), prefixed by WW, courtesy of G.W. Leo (unpub. data). All analyses were performed at the U.S. Geological Survey, Reston, Va. Major element values were determined by X-ray spectroscopy by D.F. Siems and J.E. Taggart; values for FeO, H_2O, and CO_2 were determined by X-ray spectroscopy by Hezekiah Smith, J.W. Marinenko, and J.R. Gillison. Minor element values were determined by Instrumental Neutron Activation Analysis by G.A. Wandless, P.A. Baedecker, J.S. Mee, and J.N. Grossman. —, no data]

Map symbol ➢	**Ybg**	**Ybg**	**Ym**	**Yml**	**Yg**	**Ygt**	**Yhm**	**Ypg**	**Ypg**	**Yp**	**Yp**	**Yn**	**Yn**
Sample no. ➢	**BR–554**	**P7A**	**WW–22**	**WW–29**	**BR–11**	**340 cut**	**HF2**	**J329**	**J284**	**BR–660**	**P41**	**BR–602A**	**BR–1388**
SiO_2	70.2	67.4	70.5	75.6	75.6	70.8	63.7	69.4	72.6	73.2	71.8	50.5	52.9
Al_2O_3	13.8	15.6	14.4	12.7	13	15.1	15.4	14.9	13.6	11.3	13.5	16.4	16.6
Fe_2O_3	1.72	.69	1.33	1.04	.65	.61	.95	2.68	1.47	1.1	1.2	1.84	2.1
FeO	1.8	2.2	1.2	.44	.44	1.8	3.1	.28	.4	3.4	3.3	5.6	8.2
MgO	.74	1.05	.51	.29	.22	.63	1.25	.9	.56	1.73	1.64	7.55	3.28
CaO	1.79	2.42	1.49	.53	.79	1.35	3.72	1.3	.53	1.48	2.4	11.3	7.16
Na_2O	2.68	4.23	3.39	2.9	3.41	3.55	2.78	2.41	3.03	2.72	2.52	2.48	3.45
K_2O	5.04	3.47	4.79	5.09	5.11	4.45	4.94	5.53	5.78	1.32	1.12	.9	1.01
TiO_2	.47	.6	.48	.16	.24	.26	.93	.47	.27	.67	.73	.65	1.77
P_2O_5	.18	.2	.13	.13	.05	.1	.28	.13	.12	.06	.06	.07	.58
MnO	.06	.04	.02	.02	.02	.04	.06	.03	.01	.1	.08	.13	.17
H_2O^+	.62	1.1	.59	.47	.29	.6	1.2	1.1	.53	1.7	.81	2.5	2.1
H_2O^-	.11	.05	.09	.05	.04	.07	.03	.07	.04	0	.11	.01	.12
CO_2	0	.32	.03	0	0	0	.75	0	.07	0	—	.01	.01
Total, in percent	99.21	99.37	98.95	99.42	99.86	99.36	99.09	99.2	99.01	98.78	99.27	99.94	99.45
Apatite	0.4	0.5	0.3	0.3	0.1	0.2	0.7	0.3	0.3	0.1	0.1	0.1	1.4
Ilmenite	.9	1.1	.9	.3	.5	.5	1.8	.7	.5	1.3	1.4	.9	3.5
Magnetite	2.5	1.0	1.9	1.0	.8	.9	1.4	—	.5	1.6	1.7	2.0	3.1
Orthoclase	29.8	20.5	28.3	30.1	30.2	26.3	29.2	32.6	34.1	7.8	6.6	5.4	6.1
Albite	22.7	35.8	28.7	24.5	28.9	30.1	23.5	20.4	25.6	23.0	21.3	22.7	30.0
Anorthoclase	7.7	10.7	6.5	1.8	3.6	6.1	15.0	5.6	1.8	7.0	11.5	31.6	27.6
Diopside	—	—	—	—	—	—	1.4	—	—	—	—	20.1	4.2
Hypersthene	3.1	5.2	1.6	.7	.5	4.0	5.9	2.2	1.4	8.7	8.1	14.5	17.3
Corundum	1.1	.9	1.2	1.7	.5	2.2	—	2.9	1.7	2.8	3.9	2.6	—
Quartz	30.4	22.2	28.7	38.1	34.4	28.5	18.4	30.5	31.2	44.8	43.7	—	6.7
Hematite	—	—	—	.3	.1	—	—	2.7	1.1	—	—	—	—
Rutile	—	—	—	—	—	—	—	.1	—	—	—	—	—
Total, in percent	98.6	97.9	98.1	98.8	99.6	98.8	97.3	98.0	98.2	97.1	98.3	99.9	99.9

Like the other gneisses, layered granitic gneiss (Ylg) weathers white, gray, or pink and is mostly medium grained but is distinguished by its variable texture. On an outcrop scale the textures are well foliated and gneissic, with an ill-defined, diffuse boundary between the two textural domains. Layered granitic gneiss may be a migmatite whose origin was perhaps a layered felsic volcanic rock (table 3, sample no. 19). This unit is correlated with the Stage Road layered gneiss of the central Virginia Blue Ridge (Sinha and Bartholomew, 1984). Layered granitic gneiss can be seen near Bloomfield (Southworth, 1994).

A large area of hornblende monzonite gneiss (Yhm), a gray, well-foliated rock, also has been mapped west of the Short Hill fault. Hornblende is the dominant mafic mineral (as much as 30 percent by volume), quartz content is typically only 10 to 20 percent, and microcline is as much as 50 percent by volume (table 1). Lighter colored, more leucocratic phases also are found. This type of rock is almost entirely confined to the western Blue Ridge, but a small body is found east of Hillsboro. It resembles the well-foliated granulite gneiss of the central Virginia Blue Ridge (Sinha and Bartholomew, 1984; Evans, 1991) except that hornblende and not hypersthene is the dominant mafic mineral. This unit can be seen north of Eubanks.

Two granitic gneisses (Ygt and Ym) that are abundant in the eastern Blue Ridge also are found in lesser amounts in the western Blue Ridge. Garnetiferous leucocratic metagranite (Ygt) occurs both north and south of the main body of hornblende monzonite gneiss (Yhm) and near the southern edge of Loudoun County. It can be seen as crosscutting dikes (not shown on map) in many outcrops of porphyroblastic metagranite (Ypg) (Southworth, 1994), an intrusive relation that corroborates U-Pb zircon data (table 3, sample no. 10) and may help to explain U-Pb monazite data. Garnetiferous leucocratic metagranite (Ygt) can be seen north of Loudoun Heights (Southworth and Brezinski, 1996). Pink- to orange-weathering biotite granite gneiss occurs near the town of Round Hill and is considered to be a western extension of the Marshall Metagranite (Ym).

Mesoproterozoic Metamorphism and Deformation

Although the Mesoproterozoic rocks have been extensively overprinted by subsequent Paleozoic deformation and low-grade metamorphism, Mesoproterozoic metamorphic fabrics defined by high-grade mineral assemblages and ductile structures are still clearly discernible in many places. These textures are typically granoblastic with triple-junction grain boundaries defined by mineral assemblages that are stable at granulite-facies metamorphism (for example, orthopyroxene and microcline (Yc) or orthopyroxene and brown hornblende (Yn)). Grenville structures seen in outcrop include a foliation defined by platy or tabular mafic minerals, such as biotite, or, less commonly, hornblende, and flattened quartz and feldspar grains; layering defined by concordant thin aplite or pegmatite sills; biotite streaking and rodded quartz and feldspar; and isoclinal folds in metamorphic foliation.

The Mesoproterozoic rocks record at least three episodes of deformation, beginning after the intrusion of the oldest (Group 1) granites. A well-developed, northwest-trending foliation, seen only in the western Blue Ridge and here called D_1 (fig. 3*A*, on map sheet), is found in Group 1 porphyroblastic metagranite (Ypg) and layered granitic gneiss (Ylg) and probably also in older hornblende monzonite gneiss (Yhm), but not in younger Group 2 Marshall Metagranite (Ym). Locally, D_1 is truncated by Group 3 garnetiferous leucocratic metagranite (Ygt). This constrains the age of D_1 deformation to about 1,118 to 1,110 Ma (Burton and others, 1994). Other Group 2 and Group 3 granitic gneisses have a weaker, northwest- to northeast-trending foliation, here called D_2, that must have formed after the intrusion of Group 3 gneisses (<1,055 Ma). D_2 foliation is locally accompanied by (1) southeast-plunging mineral streaking in biotite-rich rocks, (2) colinear stretching lineations in quartz and feldspar, and (3) tight isoclinal to asymmetric, southeast-plunging sheathlike folds. The D_2 lineations suggest tectonic transport to the northwest or southeast. D_3 deformation produced broad, northwest-trending folding of D_2 foliation (fig. 3*B*, on map sheet) and spreading of the orientations of D_2 lineations (fig. 3*C*, on map sheet). Map-scale D_3 folding is evident in the broad arch cored by the Marshall Metagranite south of Lovettsville and the curvilinear foliation pattern north of Waterford. Dip reversals caused by D_3 folding are shown by the west-plunging lineations shown in figure 3*C*. D_3 deformation is possibly also responsible for rare local zones of tight, north-plunging folds (fig. 3*C*) as in the small area of layered granitic gneiss (Ylg) south of Lincoln. Aplites intruding D_3 folds appear to be synkinematic and suggest that high-grade metamorphic conditions were still present in late Grenville time.

Monazite U-Pb Ages from Mesoproterozoic Rocks

Seven monazite ages, ranging from 1,127 to 1,033 Ma, were obtained from samples of biotite granite gneiss (Ybg), pink leucocratic metagranite (Yml), Marshall Metagranite (Ym), garnetiferous leucocratic metagranite (Ygt), and porphyroblastic metagranite (Ypg) (table 3). All of these ages could represent divergent local cooling ages (times when temperatures dropped below about 720 °C, the lead closure temperature for monazite) after a regional metamorphic thermal peak before 1,127 Ma. Conversely, they could represent local thermal resetting of the zircon in a given intrusive rock by subsequent intrusive events, because three of the dates are close to the crystallization ages obtained from zircon in adjacent younger intrusive rocks. The two monazite ages of 1,106 and 1,060 Ma (table 3, sample nos. (9) and (10)) for the porphyroblastic metagranite (Ypg) (zircon U-Pb age of 1,144 Ma; table 3, sample no. 17) could record intrusion of the Marshall Metagranite (Ym) and garnetiferous leucocratic metagranite (Ygt), respectively, which corroborates intrusive relations seen in the field both in and south of Loudoun County (P.T. Lyttle, oral commun., 1994). The monazite age of 1,051 Ma (table 3, sample no. (7)) for the Marshall Metagranite (zircon U-Pb ages of 1,112 and 1,111 Ma; table 3, sample nos. 13 and 12, respectively) may correspond to the intrusion of biotite granite gneiss (Ybg), although intrusive contacts between the two units have not been seen. The youngest ages (1,034 and 1,033 Ma), obtained from

Table 3. Ages related to intrusion of igneous rocks.

[Ma, million years ago. Samples not from Loudoun County are marked with an asterisk. Hbl, hornblende; WR, whole rock age; Zr, zircon crystallization age; Musc, muscovite; Phl, phlogopite; Mon, monazite]

Sample no.[1]	Map symbol	Unit	Latitude/ longitude	Technique	Age, in Ma	Reference	Sample no. for modal analysis (table 1) or geochemical analysis (table 2)
		Ages related to intrusion of igneous rocks					
1	Jdg	Diabase granophyre	39°04′/77°31′	$^{40}Ar/^{39}Ar$; Hbl	197	Kunk and others (1992).	
2	Jdl	Diabase granophyre	39°19′/77°41′	$^{40}Ar/^{39}Ar$; Hbl	200	do.	
*3	Jdh	Diabase	38°46′/77°37′	$^{40}Ar/^{39}Ar$; WR	200.3±1.2 and 201.2±1.3	Sutter (1988).	
4	Zrd	Metarhyolite dike	39°18′/77°35′	U-Pb; Zr	571.5±5	Aleinikoff and others (1995).	
5	Zcr	Catoctin Formation metarhyolite tuff	39°06′/77°49′	U-Pb; Zr	600	do.	
*6	Zrr	Robertson River Igneous Suite granite	38°53′/77°58′	U-Pb; Zr	722±3	Tollo and Aleinikoff (1992).	
		Group 3					
7	Ybg	Biotite granite gneiss	39°14′/77°36′	U-Pb; Zr	1,055±4	Aleinikoff and others (2000).	BR–554
8	Yml	Pink leucocratic metagranite	38°58′/77°47′	U-Pb; Zr	1,059±2	do.	WW–29
9	Yg	Leucocratic metagranite	39°18′/77°34′	U-Pb; Zr	1,060±2	do.	BR–11
10	Ygt	Garnetiferous leucocratic metagranite	39°19′/77°42′	U-Pb; Zr	~1,077±4	do.	340 cut
*11	Yqp	Quartz-plagioclase gneiss	39°25′/77°33′	U-Pb; Zr	1,077±4	do.	BR–36
		Group 2					
12	Ym	Marshall Metagranite	38°58′/77°45′	U-Pb; Zr	1,111±2	Aleinikoff and others (2000).	WW–22
13	Ym	Marshall Metagranite	38°59′/77°45′	U-Pb; Zr	1,112±3	do.	WW–22
		Group 1					
14	Ymc	Coarse-grained metagranite	39°03′/77°44′	U-Pb; Zr	~1,140		
15	Ypg	Porphyroblastic metagranite	39°06′/77°47′	U-Pb; Zr	~1,140		
16	Yhm	Hornblende monzonite gneiss	39°10′/77°45′	U-Pb; Zr	1,142±11		
*17	Ypg	Porphyroblastic metagranite	38°44′/77°59′	U-Pb; Zr	1,144±2		J329 and J284
18	Yhm	Hornblende monzonite gneiss	39°17′/77°44′	U-Pb; Zr	1,149±19		HF2
*19	Ylg	Layered granitic gneiss	39°57′/77°53′	U-Pb; Zr	1,153±6		

Table 3. Ages related to intrusion of igneous rocks.—Continued

[Ma, million years ago. Samples not from Loudoun County are marked with an asterisk. Hbl, hornblende; WR, whole rock age; Zr, zircon crystallization age; Musc, muscovite; Phl, phlogopite; Mon, monazite]

Sample no.[1]	Map symbol	Unit	Latitude/ longitude	Technique	Age, in Ma	Reference	Sample no. for modal analysis (table 1) or geochemical analysis (table 2)
		Ages related to regional metamorphism or granitic intrusion cooling history					
(1)	Ꞓw	Weverton Formation quartzite	39°15′/77°33′	$^{40}Ar/^{39}Ar$; Musc	350 to 300	Burton and others (1992b).	
(2)	Zcm	Catoctin Formation marble	39°01′/77°40′ and 39°15′/77°34′	$^{40}Ar/^{39}Ar$; Phl		Kunk and others (1993).	
(3)	Yc	Charnockite	39°17′/77°44′	$^{40}Ar/^{39}Ar$; Hbl	1,000–920, preferred age	do.	
(4)	Yn	Metanorite	39°13′/77°41′ and 39°59′/77°43′	$^{40}Ar/^{39}Ar$; Hbl	998	Kline and others (1994).	
(5)	Ybg	Biotite granite gneiss	39°14′/77°36′	U-Pb; Mon	1,033±2	Aleinikoff and others (2000).	
(6)	Yml	Pink leucocratic metagranite	38°58′/77°47′	U-Pb; Mon	1,034±2	do.	
(7)	Ym	Marshall Metagranite	38°59′/77°45′	U-Pb; Mon	1,051±2	do.	
(8)	Ygt	Garnetiferous leucocratic metagranite	39°19′/77°42′	U-Pb; Mon	1,070±3	do.	
*(9)	Ypg	Porphyroblastic metagranite	38°44′/77°59′	U-Pb; Mon	1,106±1	do.	
(10)	Ypg	Porphyroblastic metagranite	39°06′/77°47′	U-Pb; Mon	1,127±1 and 1,060±1	do.	

[1]Sample locations are shown on map sheet (fig. 1 and the map).

pink leucocratic metagranite (Yml) and biotite granite gneiss (Ybg), respectively (table 3, sample nos. (6) and (5)), may represent final cooling from regional metamorphism. However, the existence of monazites with preserved older ages indicates that there was no regional thermal event with temperatures greater than 720 °C that affected all of these rocks in late Grenville time and that intrusion and deformation of Group 2 and Group 3 granites occurred within a temperature interval defined by the minimum melt temperature for water-saturated rocks and the closure temperature of monazite (~650 to 720 °C).

Hornblende-bearing gneisses (Yc, Yn) were analyzed to obtain hornblende cooling ages by the $^{40}Ar/^{39}Ar$ technique (table 3, sample nos. (3) and (4)). The resulting spectra are all discordant but suggest cooling ages in the range of 1,000 to 920 Ma (Kunk and others, 1993). A 998-Ma cooling age for igneous hornblende of the metanorite (Yn on the map) north of Middleburg was reported by Kline and others (1994). This age range represents the period in which regional temperatures fell below about 500 °C (argon closure temperature for hornblende) at the end of the Grenville orogeny. Therefore 1 Ga can be considered to be a minimum age for development of Mesoproterozoic structures and mineral assemblages in the northern Blue Ridge anticlinorium.

Summary of Mesoproterozoic Geologic Events

Isotopic and structural data from the Mesoproterozoic rocks record a rich history of plutonism, deformation, and metamorphism in the period from 1,153 to about 1,000 Ma, a span of more than 150 million years (Burton and Southworth, 2004). At least three episodes of granitic intrusion and crystallization occurred beginning around 1,144 Ma, accompanied and followed by several episodes of deformation that produced ductile folds and regional foliations and lineations. The deformation and accompanying metamorphic recrystallization ended no earlier than about 1,033 Ma, the crystallization age of biotite granite gneiss (Ybg), which has a well-developed foliation, lineations, and folds. Rare, late undeformed pegmatites cut these structures and thus are younger. Grenvillian activity ceased by about 1,000 Ma, at which time temperatures dropped below about 500 °C, the argon closure temperature for hornblende.

Late Proterozoic Granite

In the extreme southwestern corner of the county a body of granite marks the northernmost termination of the Robertson River Igneous Suite, a narrow, 70-mile (mi)-long, northeast-trending belt of Late Proterozoic granitic rocks. The Robertson River Igneous Suite has been subdivided into nine units of peralkaline to metaluminous granite and syenite (Tollo and others, 1991; Tollo and Lowe, 1994). The granite exposed in Loudoun County is part of the Cobbler Mountain Alkali Feldspar Quartz Syenite (Zrr). The syenite is composed of stubby, euhedral mesoperthite crystals 0.04 to 0.08 in. in diameter intergrown with anhedral quartz and minor interstitial plagioclase, in addition to a mafic phase (amphibole?) that has been broken down into quartz, plagioclase, and magnetite. In outcrop it is a distinctive, medium- to coarse-grained, massive rock in which the perthite crystals are conspicuous on the tan-weathered surface. It has been dated as Late Proterozoic in age (~722 Ma) (table 3, sample no. 6) and lacks the Grenville foliation of the surrounding basement gneisses. The rocks of the Robertson River Igneous Suite have compositions typical of anorogenic granites (Tollo and others, 1991); they may represent an older stage of Iapetan rifting that also produced the felsic volcanic rocks of the Mount Rogers Formation of southwestern Virginia, the Crossnore Complex of central Virginia, and the Bakersville Gabbro of North Carolina (Rankin and others, 1989).

Late Proterozoic Dikes

Intruding the Mesoproterozoic and Late Proterozoic granitic rocks is a northeast-trending swarm of tabular dikes (Zmd) that commonly range in width from a few inches to tens of feet and are diabase (greenstone) in composition. The dikes were extensively recrystallized and deformed in varying degrees during the Paleozoic deformation that produced the Blue Ridge anticlinorium. They can be grouped texturally and compositionally into three types in descending abundance: fine-grained metadiabase (by far the most common type) and coarse-grained and porphyritic metadiabase (both mapped as Zmd) and metarhyolite (Zrd). The bimodal nature of the compositions of the dikes suggests that they were feeders to the overlying rocks of the Catoctin Formation, which consists of voluminous metabasalts and minor metarhyolites—a conclusion reached by many workers (for example, Stose and Stose, 1946; Reed, 1955; Nickelsen, 1956; Espenshade, 1986; Southworth, 1991; Burton and others, 1995).

Dike Composition

The fine-grained, dark-green-weathering metadiabase dikes (Zmd) are primarily composed of chlorite, epidote, and altered plagioclase (albite). Greenish-brown biotite, stilpnomelane, and pale-green amphibole (actinolite) in tabular or needle form also are found. This mineral assemblage is typical for a rock of basaltic composition that was metamorphosed under lower greenschist-facies conditions. Paleozoic cleavage, defined by chlorite and muscovite, is weakly to strongly developed in the greenstone dikes and results in textures ranging from massive greenstone to greenschist. In the coarse-grained metadiabase dikes (shown by a pattern north of Taylorstown) the mineral assemblage is similar, except that actinolite is the most abundant mineral, making up 50 to 70 percent of the rock in the form of subequant crystals that are 0.08 to 0.16 in long. In outcrop the coarse-grained dikes have a distinctive nubbly surface texture due to weathering out of the large amphiboles, in contrast to the smoother weathering surface of the fine-grained dikes. The stubby, equant character of the actinolite in the coarse-grained dikes suggests that it is derived from primary igneous pyroxene. Porphyritic metadiabase dikes (not differentiated on the map) contain abundant relict white to pink subhedral phenocrysts of plagioclase (now heavily saussuritized), 0.04 to 0.2 in long in a fine-grained groundmass of actinolite, chlorite, and epidote.

Metarhyolite dikes (Zrd) are gray-weathering, fine-grained but locally porphyritic, and commonly have a well-developed Paleozoic cleavage. In thin section they have a fine-grained, felty texture composed of microcrystalline quartz and potassium feldspar surrounding scattered larger rounded grains of plagioclase. Several of these dikes have been mapped, including a large one that is 33 to 66 feet (ft) thick and extends 8.7 mi south from the Potomac River (Southworth, 1991, 1995). North of the Potomac River, Fauth and Brezinski (1994) report similar felsic dikes that intrude basement gneiss and, locally, rocks of the lower part of the Catoctin Formation. Zircons from a smaller metarhyolite dike exposed along the Potomac River (Burton and others, 1995) yielded a U-Pb date of 571.5±5 Ma (table 3, sample no. 4).

Dike Orientation and Density

The Late Proterozoic dikes were intruded into the crust in a northeast orientation with steep dips, in accordance with a northwest extension direction and lateral spreading during the opening of Iapetus Ocean (Rankin, 1975). Poles to dike contacts and azimuthal trends of well-exposed dikes along Catoctin Creek (Burton and others, 1995) (fig. 3*D* and *E*, on map sheet) are representative of dike orientations for this region. Dike contacts are subparallel to the dominant Paleozoic cleavage, suggesting either transposition of the dikes into parallelism with regional cleavage (Southworth, 1991), reactivation of previously existing dike-basement contacts by developing cleavage, or both.

Along the Potomac bluffs, the metadiabase dikes constitute from 50 percent (Southworth, 1991) to 60 percent (Burton and others, 1995) of the exposed rock as measured across strike. Assuming that dike emplacement was by forceful intrusion and dilation rather than stoping and assimilation, this locally implies a crustal extension of 150 percent. In a pipeline trench near the southern edge of the county, south of St. Louis, Espenshade (1983) found that Late Proterozoic metadiabase dikes make up about 20 percent of the basement. This suggests that overall dike density increases northward. In areas of poor exposure, soil, rock chips, and well cuttings suggest that the dikes are undoubtedly more abundant than shown on the map.

Geochemical Relation of Metadiabase Dikes to Metabasalt of the Catoctin Formation

Comparison of major and minor element geochemical analyses of metadiabase dikes (table 4) and metabasalts of the Catoctin Formation (table 5) demonstrates the probable relation of the feeder dikes to the extrusive flows (fig. 4*A–E* , on map sheet). Lack of extensive veining and wall-rock alteration suggests that the dikes behaved as relatively closed (isochemical) systems during metamorphism. In contrast, the presence of epidosite (epidote-quartz rock) lenses and layers in Catoctin Formation metabasalt indicates that it was locally subjected to chemical migration during metamorphism (Reed and Morgan, 1971). Figure 4 shows geochemical plots of the three types of metadiabase dikes in comparison with metabasalt of the Catoctin Formation. Also shown are the texturally and chemically distinct, low TiO_2/high MgO metavolcanic flows and flow breccias first noted by Espenshade (1986) south of Loudoun County. Both Espenshade (1986) and P.T. Lyttle (oral commun., 1993) have mapped these breccias at or near the base of the Catoctin; they apparently do not extend north into Loudoun County, and intrusive (dike) equivalents of these rocks have not been found. An AFM diagram (fig. 4*A*) indicates that the mafic rocks are mostly of tholeiitic basalt composition. In major element variation diagrams (fig. 4*B–D*) the coarse-grained metadiabase dikes and the porphyritic metadiabase dikes appear to occupy distinct, separate fields that are each smaller than but largely overlap the field for the fine-grained metadiabase dikes. The fields for the fine-grained metadiabase dikes and the metabasalts of the Catoctin Formation are quite similar; the large scatter of a few metabasalt samples may be due to metamorphic alteration. The dikes and metabasalt are thus basically identical with respect to major elements and belong to the high TiO_2/low MgO suite of Espenshade (1986).

The rocks of the low TiO_2/high MgO suite of Espenshade (1986) have distinctive, low rare earth element (REE) values with a shallow slope (fig. 4*E*). The REE abundances of the coarse-grained dikes are more elevated than those of the low TiO_2/high MgO suite but occupy a range that is narrower and generally more depleted in light rare earth elements. The fine-grained and porphyritic dikes have ranges of REE abundances that closely resemble the range for the metabasalts of the Catoctin Formation. Both the major and minor element data, therefore, indicate that the metadiabase dikes and metabasalt flows of the Catoctin Formation are geochemically equivalent. Espenshade (1986) considered the rocks of his low TiO_2/high MgO suite to represent products of relatively undifferentiated early magmas. The distinct fields on variation diagrams (fig. 4*B–D*) for the coarse-grained dikes and the porphyritic dikes may be indications of slight magma differentiation during the main phase of dike intrusion and basalt eruption of rocks of the Catoctin Formation.

U-Pb Age of Rhyolite Dike

Zircons from a small metarhyolite dike along the Potomac River (Burton and others, 1995) were analyzed by the U-Pb isotopic method and yielded an age of 571.5±5 Ma (table 3, sample no. 4). The dike cuts an adjacent metadiabase dike, thus establishing a minimum age for the latter. The metarhyolite dike age represents a reasonable age for metarhyolite flows (Zcr) in the overlying Catoctin Formation and is in agreement with the 570±36 Ma age of Badger and Sinha (1988).

Late Proterozoic Metasedimentary and Metavolcanic Rocks

Nonconformably overlying the basement gneisses is a variegated basal sequence of clastic metasedimentary rocks of the Fauquier and Swift Run Formations. Rocks of the two formations are not in contact, but they occupy the same stratigraphic position between the Mesoproterozoic gneisses and the overlying Late Proterozoic Catoctin Formation. Rocks of the Fauquier Formation are confined to the southern part of the east limb of the Blue Ridge anticlinorium and are generally coarser grained than rocks of the Swift Run Formation. The Fauquier Formation can be traced northward from the Fauquier County line to near Beaverdam Creek and Mountville where it is terminated against Mesoproterozoic rocks along a down-to-the-south normal fault. The Swift Run Formation can be traced south from the Potomac River to just north of Hughesville (spelled incorrectly as Hugesville on base map), where it is terminated against Mesoproterozoic rocks along a down-to-the-north normal fault. Between the normal faults, rocks of the Catoctin Formation unconformably overlie the basement gneisses. The faults are considered to be synsedimentary and rift-related, and hence Late Proterozoic in age (Kline and others, 1991), and probably influenced the distribution of the strata that distinguish the two formations. Although rocks of the Fauquier Formation, the Lynchburg Group, the Mechum River Formation, and the Swift Run Formation all occupy the same stratigraphic position immediately above the crystalline basement, they need not be exact time-stratigraphic correlatives (Rader and Evans, 1993) due to the separateness and possible diachroneity of the rift basins.

Fauquier Formation

The Fauquier Formation (Furcron, 1939; Espenshade, 1986) consists of a broadly upward-fining sequence of basal metaconglomerate and meta-arkose (Zfc), crossbedded meta-arkose (Zfa), and rhythmically bedded metasiltstone and metamudstone (Zfs). The thickness of the Fauquier Formation varies widely (0–1,500 ft) over a relatively short distance along strike which, combined with its locally coarse grain size, suggests that the formation was deposited in local fault-bounded

Table 4. Major and minor element geochemical analyses of Late Proterozoic metadiabase dikes.

[Sample locations with the prefix BR are found in Burton and others (1995), sample locations with the prefixes B, P, and HF are found in Southworth (1994, 1995) and Southworth and Brezinski (1996), and sample locations with the prefixes LN and RD are from J.S. Schindler (unpub. data). All analyses were performed at the U.S. Geological Survey, Reston, Va. Major element values were determined by X-ray spectroscopy by D.F. Siems and J.E Taggart; values for FeO, H_2O, and CO_2 were determined by X-ray spectroscopy by Hezekiah Smith, J.W. Marinenko, and J.R. Gillison. Minor element values were determined by Instrumental Neutron Activation Analysis by G.A. Wandless, P.A. Baedecker, J.S. Mee, and J.N. Grossman. Major element values are given in weight percent, and minor element values are given in parts per million. —, no data]

Dike type ➢	Porphyritic	Porphyritic	Porphyritic	Porphyritic	Porphyritic	Porphyritic	Porphyritic	Porphyritic	Porphyritic	Porphyritic	Coarse-grained	Coarse-grained
Sample no. ➢	**BR–681**	**B1**	**HF15**	**P3**	**LN–116**	**LN–123**	**LN–154**	**LN–253**	**LN–256**	**LN–269**	**BR–2**	**BR–67**
SiO_2	48.70	48.20	44.60	47.90	47.40	49.30	47.90	48.40	46.60	47.10	45.40	44.60
TiO_2	1.34	1.58	1.20	1.90	1.97	2.24	1.63	2.10	3.40	1.91	1.98	2.31
Al_2O_3	17.40	16.20	16.90	16.00	15.70	14.80	16.30	14.60	12.10	15.70	14.50	14.00
Fe_2O_3	2.97	3.03	6.10	3.67	4.72	2.55	3.44	3.42	5.46	3.75	3.80	3.74
FeO	6.20	7.00	5.00	7.60	7.10	9.50	6.90	8.90	10.40	7.70	9.10	10.50
MnO	.15	.15	.16	.17	.18	.19	.16	.20	.26	.18	.20	.24
MgO	5.61	6.34	4.96	5.57	6.30	5.31	6.21	6.28	5.02	6.20	7.67	6.97
CaO	11.30	11.90	18.40	10.90	11.50	10.50	11.20	10.40	8.62	11.10	11.10	10.30
Na_2O	3.01	1.79	.84	2.59	2.41	2.59	2.41	2.55	.73	2.22	1.81	2.54
K_2O	.47	.76	.14	.53	.52	.77	1.06	.66	3.70	.48	.78	.20
H_2O^+	2.80	3.10	1.10	2.80	1.40	1.40	2.00	1.80	2.60	2.90	2.80	2.90
H_2O^-	.03	.12	.19	.21	.21	.05	.12	.08	.19	.20	.20	.03
P_2O_5	.15	.15	.17	.25	.23	.25	.17	.30	.64	.25	.18	.32
CO_2	.01	<.01	.01	.02	.02	.01	0	.01	.01	.01	.01	.01
Total, in percent	100.14	100.33	99.77	100.11	99.66	99.46	99.50	99.70	99.73	99.70	99.53	98.66
Scandium	29.3	30.2	32.6	31.8	35.9	30.6	32	37.7	39.9	34.3	39.1	38.2
Chromium	154	196	154	158	194	48.8	138	210	47.2	207	163	72.1
Cobalt	31.4	47.2	27.9	36.3	41.5	44.8	40.4	44.7	44.6	43.2	51.1	51
Nickel	35	92	79	65	66	52	95	77	<31	75	104	92
Zinc	78.7	89	66	106	92	89	70	120	160	110	77	93
Arsenic	<.7	16.8	1.02	<.6	<1.5	<1.5	<1.1	<.7	<.5	.8	<1	<.9
Selenium	<.7	<2	1	<.7	—	—	—	—	—	—	<2	<3

Table 4. Major and minor element geochemical analyses of Late Proterozoic metadiabase dikes.—Continued

[Sample locations with the prefix BR are found in Burton and others (1995), sample locations with the prefixes B, P, and HF are found in Southworth (1994, 1995) and Southworth and Brezinski (1996), and sample locations with the prefixes LN and RD are from J.S. Schindler (unpub. data). All analyses were performed at the U.S. Geological Survey, Reston, Va. Major element values were determined by X-ray spectroscopy by D.F. Siems and J.E Taggart; values for FeO, H_2O, and CO_2 were determined by X-ray spectroscopy by Hezekiah Smith, J.W. Marinenko, and J.R. Gillison. Minor element values were determined by Instrumental Neutron Activation Analysis by G.A. Wandless, P.A. Baedecker, J.S. Mee, and J.N. Grossman. Major element values are given in weight percent, and minor element values are given in parts per million. —, no data]

Dike type ➢	**Porphyritic**	**Porphyritic**	**Porphyritic**	**Porphyritic**	**Porphyritic**	**Porphyritic**	**Porphyritic**	**Porphyritic**	**Porphyritic**	**Porphyritic**	**Coarse-grained**	**Coarse-grained**
Sample no. ➢	**BR–681**	**B1**	**HF15**	**P3**	**LN–116**	**LN–123**	**LN–154**	**LN–253**	**LN–256**	**LN–269**	**BR–2**	**BR–67**
Rubidium	12	48.3	8.2	22.6	30	44	32	26	188	25	20	<7
Strontium	430	310	779	320	400	330	430	320	350	350	446	330
Zirconium	140	160	70	200	120	180	170	150	250	130	190	160
Molybdenum	<5	<4	4	<5	—	—	—	—	—	—	<4	<7
Antimony	<.09	<.1	.07	<.2	<.12	<.11	<.11	<.1	.1	<.1	<.1	<.1
Cesium	<.2	<.5	.2	<.2	<.5	.31	<.17	.31	.71	.58	<.2	<.2
Barium	159	82	80	230	180	220	460	220	510	130	396	<50
Lanthanum	10.31	8.7	5.66	14.6	12	16	10	16	21	12	5.76	9.9
Cerium	22.5	19.5	11.8	31.8	27.6	34.1	22	35.7	49	26.9	13.7	22.4
Neodymium	13.3	11.3	9.3	20.7	15	18	15	23	30	15	10.2	17.3
Samarium	3.6	3.53	2.47	5.5	4.83	5.4	3.79	6.12	9.08	4.84	3.48	5.51
Europium	1.22	1.19	1.71	1.67	1.66	1.78	1.32	1.87	3.02	1.61	1.33	1.93
Terbium	.65	.65	.527	.89	.91	.88	.72	.991	1.5	.76	.683	1.009
Ytterbium	2.07	1.73	1.99	2.88	2.5	2.4	1.8	3.2	4.94	2.7	2.24	3.14
Lutetium	.268	.247	.274	.389	.39	.34	.26	.44	.676	.36	.316	.449
Hafnium	2.67	2.48	1.23	3.76	3.46	4.02	2.54	4.35	5.62	3.38	2.04	3.46
Tantalum	.64	.64	.22	.82	.72	1	.74	.96	1.3	.74	.414	.525
Gold	<2	<10	<4	<9	<2.2	<8	<5	<2	6.5	<9	<1	<6
Thorium	.95	.75	<.1	1.17	.8	1.7	.88	1.2	1.3	.69	.44	.39
Uranium	.2	<.3	<.3	.29	<.15	.36	<.19	.33	.39	.18	<.2	<.4

Table 4. Major and minor element geochemical analyses of Late Proterozoic metadiabase dikes.—Continued

[Sample locations with the prefix BR are found in Burton and others (1995), sample locations with the prefixes B, P, and HF are found in Southworth (1994, 1995) and Southworth and Brezinski (1996), and sample locations with the prefixes LN and RD are from J.S. Schindler (unpub. data). All analyses were performed at the U.S. Geological Survey, Reston, Va. Major element values were determined by X-ray spectroscopy by D.F. Siems and J.E Taggart; values for FeO, H_2O, and CO_2 were determined by X-ray spectroscopy by Hezekiah Smith, J.W. Marinenko, and J.R. Gillison. Minor element values were determined by Instrumental Neutron Activation Analysis by G.A. Wandless, P.A. Baedecker, J.S. Mee, and J.N. Grossman. Major element values are given in weight percent, and minor element values are given in parts per million. —, no data]

Dike type ➢	Coarse-grained	Coarse-grained	Coarse-grained	Coarse-grained	Fine-grained	Fine-grained	Fine-grained	Fine-grained	Fine-grained	Fine-grained	Fine-grained	Fine-grained
Sample no. ➢	**BR–82**	**BR–452A**	**BR–738**	**LN–257**	**BR–452B**	**BR–226**	**BR–610A**	**HF6**	**HF7**	**HF8**	**HF9**	**HF10**
SiO_2	46.40	46.80	46.90	45.70	46.70	46.10	48.60	48.80	50.50	47.60	50.10	48.40
TiO_2	2.18	2.42	1.97	2.29	2.53	2.18	2.62	2.47	2.80	2.29	2.30	2.23
Al_2O_3	14.00	13.70	15.10	14.30	13.50	13.90	13.50	13.30	12.60	13.70	13.50	13.50
Fe_2O_3	3.76	3.61	3.42	4.12	3.83	2.53	2.51	3.44	4.86	3.76	2.60	2.86
FeO	9.40	9.90	8.90	8.90	9.70	10.60	11.70	9.60	9.40	9.40	10.00	10.40
MnO	.22	.22	.20	.21	.22	.22	.22	.20	.22	.19	.21	.22
MgO	6.92	6.47	6.55	7.15	6.11	6.94	5.56	5.83	4.36	6.29	6.14	6.38
CaO	11.20	10.40	11.00	10.80	10.70	11.20	10.50	9.59	8.73	9.54	8.80	9.54
Na_2O	2.47	2.76	2.69	1.94	2.76	2.54	2.39	2.44	2.24	3.13	2.39	2.99
K_2O	.12	.36	.26	.71	.45	.12	.71	1.42	.83	.44	.45	.64
H_2O^+	2.50	2.10	3.20	2.40	2.10	2.20	1.40	2.30	2.60	2.50	2.80	2.50
H_2O^-	.06	.01	.02	.37	.06	.09	.04	.20	.35	.29	.24	.14
P_2O_5	.23	.36	.24	.35	.34	.24	.30	.30	.35	.26	.28	.23
CO_2	0	0	.01	.01	0	0	.01	.01	.01	.01	.07	.01
Total, in percent	99.46	99.11	100.46	99.25	99.00	98.86	100.06	99.90	99.85	99.40	99.88	100.04
Scandium	40.8	43.6	37.6	39.4	41.9	38.9	35.9	33	31.2	33.9	33.9	39.7
Chromium	182	207	159	240	153	139	37.7	78.6	28.7	151	90.9	90.6
Cobalt	42.9	44.5	39.3	48.9	42.2	43.9	50	41.8	40	42	39.7	47.7
Nickel	89	78	71	87	62	89	56	53	50	63	80	83
Zinc	78.8	85	105	140	90	84	125	126	148	106	138	116
Arsenic	4.5	<1	<.7	<1	<2	<1	1.04	.5	.6	1	.6	<1
Selenium	<1	<2	<5	—	<2	<2	<4	7	5	2	3	—

Table 4. Major and minor element geochemical analyses of Late Proterozoic metadiabase dikes.—Continued

[Sample locations with the prefix BR are found in Burton and others (1995), sample locations with the prefixes B, P, and HF are found in Southworth (1994, 1995) and Southworth and Brezinski (1996), and sample locations with the prefixes LN and RD are from J.S. Schindler (unpub. data). All analyses were performed at the U.S. Geological Survey, Reston, Va. Major element values were determined by X-ray spectroscopy by D.F. Siems and J.E Taggart; values for FeO, H_2O, and CO_2 were determined by X-ray spectroscopy by Hezekiah Smith, J.W. Marinenko, and J.R. Gillison. Minor element values were determined by Instrumental Neutron Activation Analysis by G.A. Wandless, P.A. Baedecker, J.S. Mee, and J.N. Grossman. Major element values are given in weight percent, and minor element values are given in parts per million. —, no data]

Dike type ➢	**Coarse-grained**	**Coarse-grained**	**Coarse-grained**	**Coarse-grained**	**Fine-grained**	**Fine-grained**	**Fine-grained**	**Fine-grained**	**Fine-grained**	**Fine-grained**	**Fine-grained**	**Fine-grained**
Sample no. ➢	**BR–82**	**BR–452A**	**BR–738**	**LN–257**	**BR–452B**	**BR–226**	**BR–610A**	**HF6**	**HF7**	**HF8**	**HF9**	**HF10**
Rubidium	<7	16.7	7.5	29	17	14.4	26	88	43.9	24.2	11.7	24.7
Strontium	320	330	370	310	350	300	330	454	535	377	420	290
Zirconium	<200	151	<500	89	<260	125	<500	150	250	290	280	210
Molybdenum	<6	<4	<7	—	<5	<5	5.4	3.1	3.6	3.4	<4	<7
Antimony	<.1	<.1	.12	<.12	<.1	<.1	<.08	.2	.07	.09	.08	<.1
Cesium	<.2	<.2	<.3	.36	<.2	<.2	.87	1.3	1	.43	.02	<.2
Barium	117	128	93	290	157	198	204	298	290	416	374	237
Lanthanum	8.6	10.07	8.34	11	14.7	14.4	17	17.4	24.1	17.6	14.4	13.8
Cerium	19.6	24.4	20.1	23	32.1	31.1	37.7	37.3	51.2	34.1	33.7	30
Neodymium	13.6	16.7	14.2	17	20.5	19.8	23.3	26	29.4	22	21.6	18.1
Samarium	4.45	5.24	4.4	5	5.89	5.92	6.27	6.33	7.49	6.24	6.02	5.24
Europium	1.62	1.95	1.59	1.82	2.02	1.98	1.86	1.98	2.15	1.93	1.69	1.66
Terbium	.84	.976	.83	.87	1.07	1.053	.97	1.022	1.14	1.047	1.048	.96
Ytterbium	2.71	3.19	2.8	2.8	3.14	3.41	3.1	3.21	3.77	2.96	3.19	2.93
Lutetium	.381	.428	.398	.38	.461	.468	.432	.434	.516	.407	.43	.404
Hafnium	2.84	3.27	2.96	2.95	3.78	3.86	4.46	4.5	5.54	3.94	4.39	3.78
Tantalum	.53	.63	.53	.62	.82	.86	1.27	1.07	1.32	1.02	.94	.95
Gold	<8	<2	<2	<2	<2	<2	7.8	<6	<6	<.7	<2	<5
Thorium	.52	.51	.55	.47	1.09	.93	1.5	1.46	2.06	1.31	1.04	1.26
Uranium	.72	<.2	<.3	.21	.42	.31	.45	.41	.73	.41	.27	.48

Table 4. Major and minor element geochemical analyses of Late Proterozoic metadiabase dikes.—Continued

[Sample locations with the prefix BR are found in Burton and others (1995), sample locations with the prefixes B, P, and HF are found in Southworth (1994, 1995) and Southworth and Brezinski (1996), and sample locations with the prefixes LN and RD are from J.S. Schindler (unpub. data). All analyses were performed at the U.S. Geological Survey, Reston, Va. Major element values were determined by X-ray spectroscopy by D.F. Siems and J.E Taggart; values for FeO, H_2O, and CO_2 were determined by X-ray spectroscopy by Hezekiah Smith, J.W. Marinenko, and J.R. Gillison. Minor element values were determined by Instrumental Neutron Activation Analysis by G.A. Wandless, P.A. Baedecker, J.S. Mee, and J.N. Grossman. Major element values are given in weight percent, and minor element values are given in parts per million. —, no data]

Dike type ➤	Fine-grained	Fine-grained	Fine-grained	Fine-grained	Fine-grained	Fine-grained	Fine-grained	Fine-grained	Fine-grained	Fine-grained	Fine-grained	Fine-grained
Sample no. ➤	**HF11**	**HF12**	**HF13**	**P2**	**P4**	**P5**	**P6**	**P7**	**LN–121**	**LN–130**	**RD–49**	**LN–251**
SiO_2	50.50	49.30	45.80	47.90	47.90	45.60	47.30	46.90	46.70	52.10	50.10	46.60
TiO_2	2.74	1.92	3.99	2.21	1.99	1.65	2.35	1.86	2.15	1.10	2.93	2.28
Al_2O_3	13.10	13.70	12.60	14.50	13.60	16.10	12.90	14.40	14.00	13.30	12.80	14.30
Fe_2O_3	3.23	3.77	3.84	3.15	3.10	2.97	3.29	3.88	3.24	3.61	3.83	2.80
FeO	9.70	8.30	11.50	9.50	9.10	8.50	10.10	8.40	9.60	9.00	10.60	10.00
MnO	.20	.20	.24	.20	.19	.17	.21	.19	.21	.20	.22	.20
MgO	4.16	6.18	5.67	5.61	6.95	7.89	6.26	7.15	7.39	5.18	4.00	7.20
CaO	9.39	9.58	9.56	10.50	11.50	10.60	11.90	12.40	11.50	6.08	8.51	11.20
Na_2O	1.74	3.47	2.63	2.66	2.31	2.05	2.01	1.81	2.31	4.11	2.32	2.23
K_2O	.49	.39	1.30	.45	.62	.74	.70	3.50	.38	1.39	1.10	.50
H_2O^+	2.90	2.10	1.90	2.90	2.50	3.30	2.40	2.50	1.90	2.20	2.40	2.20
H_2O^-	.10	.25	.13	.19	.12	.19	.23	.14	.12	.83	.20	.01
P_2O_5	.52	.30	.53	.30	.21	.23	.21	.22	.29	.20	.49	.34
CO_2	.70	.01	.01	.02	.02	.02	.29	.02	0	.10	.01	.01
Total, in percent	99.47	99.47	99.70	100.09	100.11	100.01	100.15	103.37	99.79	99.40	99.51	99.87
Scandium	28.4	38.8	32	36.9	38.5	30.5	41.3	40.6	41.3	43	31.9	39
Chromium	32.8	124	91.1	136	222	72.8	87.5	197	233	17	17	240
Cobalt	37	42.3	51.8	38.9	45.3	46.6	45.6	51.7	54.2	43.2	40.9	48.7
Nickel	27	103	<150	47	91	109	72	105	130	<25	55	79
Zinc	147	108	142	121	113	92	120	108	96	62	130	110
Arsenic	<1	<1	<2	<.7	1.4	1.06	<1	<.6	<1.9	<3.00	1.8	<.5
Selenium	—	—	—	<3	<3	<.1	<.2	<4	—	—	—	—

Table 4. Major and minor element geochemical analyses of Late Proterozoic metadiabase dikes.—Continued

[Sample locations with the prefix BR are found in Burton and others (1995), sample locations with the prefixes B, P, and HF are found in Southworth (1994, 1995) and Southworth and Brezinski (1996), and sample locations with the prefixes LN and RD are from J.S. Schindler (unpub. data). All analyses were performed at the U.S. Geological Survey, Reston, Va. Major element values were determined by X-ray spectroscopy by D.F. Siems and J.E Taggart; values for FeO, H_2O, and CO_2 were determined by X-ray spectroscopy by Hezekiah Smith, J.W. Marinenko, and J.R. Gillison. Minor element values were determined by Instrumental Neutron Activation Analysis by G.A. Wandless, P.A. Baedecker, J.S. Mee, and J.N. Grossman. Major element values are given in weight percent, and minor element values are given in parts per million. —, no data]

Dike type ➢	Fine-grained	Fine-grained	Fine-grained	Fine-grained	Fine-grained	Fine-grained	Fine-grained	Fine-grained	Fine-grained	Fine-grained	Fine-grained	Fine-grained
Sample no. ➢	**HF11**	**HF12**	**HF13**	**P2**	**P4**	**P5**	**P6**	**P7**	**LN–121**	**LN–130**	**RD–49**	**LN–251**
Rubidium	15.8	15.1	48	18	22.9	18	25.3	13.2	20	46	100	18
Strontium	510	330	420	320	310	400	410	285	370	290	340	310
Zirconium	270	210	290	170	<400	<190	190	<60	<300	<270	330	130
Molybdenum	<6	<7	<5	<5	<6	<5	<4	<6	—	—	—	—
Antimony	.16	<.1	.21	<.1	<.09	<.09	<.2	<.09	<.12	<.5	<.06	<.1
Cesium	<.2	<.2	.4	<.2	<.2	<.3	<.3	<.2	.21	.33	2	<.21
Barium	572	163	429	125	112	290	191	141	180	410	200	170
Lanthanum	28.4	16	29.7	18.7	14.9	8.2	12.8	6.57	8.6	12	30.3	9.8
Cerium	59.8	35.1	63.7	38.4	32.7	19.2	29.3	16.2	20	25	64.8	22.4
Neodymium	34.4	18.1	35.1	23.2	19	12.8	17.4	12.8	13	14	35	15
Samarium	8.81	5.18	8.81	6.08	5.28	3.87	4.95	3.72	4.2	3.82	9.21	4.72
Europium	2.46	1.65	2.71	1.91	1.62	1.38	1.64	1.39	1.68	1.23	2.62	1.8
Terbium	1.33	.89	1.27	1.048	.89	.708	1.04	.786	.9	.75	1.51	.85
Ytterbium	3.87	2.85	3.02	3.21	2.64	2.29	3.08	2.58	2.6	3	4.2	2.7
Lutetium	.53	.386	.404	.483	.39	.342	.45	.365	.37	.46	.6	.37
Hafnium	6.45	3.93	5.49	4.43	3.76	2.55	3.85	2.16	2.7	2.6	7.11	2.95
Tantalum	1.3	.99	2.24	.93	.96	.485	1.03	.43	.48	.38	1.54	.6
Gold	<4	<5	<7	—	<9	<3	<4	<2	<2.4	<1.9	<5	<2.8
Thorium	1.83	2.09	3.17	1.33	1.62	.33	1.48	.33	.49	2.3	2.4	.46
Uranium	.66	.73	1.1	.29	.38	<.7	.4	<.3	<.23	.61	.64	.19

Table 4. Major and minor element geochemical analyses of Late Proterozoic metadiabase dikes.—Continued

[Sample locations with the prefix BR are found in Burton and others (1995), sample locations with the prefixes B, P, and HF are found in Southworth (1994, 1995) and Southworth and Brezinski (1996), and sample locations with the prefixes LN and RD are from J.S. Schindler (unpub. data). All analyses were performed at the U.S. Geological Survey, Reston, Va. Major element values were determined by X-ray spectroscopy by D.F. Siems and J.E Taggart; values for FeO, H_2O, and CO_2 were determined by X-ray spectroscopy by Hezekiah Smith, J.W. Marinenko, and J.R. Gillison. Minor element values were determined by Instrumental Neutron Activation Analysis by G.A. Wandless, P.A. Baedecker, J.S. Mee, and J.N. Grossman. Major element values are given in weight percent, and minor element values are given in parts per million. —, no data]

Dike type ➢	Fine-grained	Fine-grained	Fine-grained	Fine-grained	Fine-grained	Fine-grained	Fine-grained	Fine-grained	Fine-grained	Fine-grained
Sample no. ➢	**LN–252**	**LN–258**	**LN–261**	**LN–268**	**LN–270**	**LN–273**	**LN–276**	**LN–292A**	**LN–292B**	**LN–317**
SiO_2	46.70	48.40	48.60	47.30	48.70	49.00	46.00	41.70	44.00	50.40
TiO_2	1.21	2.83	2.55	1.90	3.02	3.11	2.24	4.00	3.70	2.81
Al_2O_3	16.00	13.20	14.00	14.00	12.80	12.60	14.20	13.40	12.70	12.90
Fe_2O_3	2.29	2.76	3.33	3.12	3.61	4.73	4.05	4.70	6.55	4.43
FeO	8.30	11.30	10.60	9.80	11.70	9.70	8.60	11.80	10.50	9.70
MnO	.18	.22	.22	.21	.23	.21	.19	.26	.25	.21
MgO	8.44	5.54	4.87	7.00	4.37	4.63	7.12	5.98	5.33	4.27
CaO	11.60	10.30	9.79	11.00	8.99	8.75	11.00	11.90	9.21	7.80
Na_2O	2.08	2.23	2.32	2.26	2.48	2.44	1.62	1.85	1.82	2.80
K_2O	.28	.73	.93	.52	.92	.96	1.18	.27	1.17	1.23
H_2O^+	2.40	1.60	1.90	2.30	2.30	2.50	3.10	3.20	3.20	2.60
H_2O^-	.13	.17	.13	.10	.22	.30	.14	.12	.36	.24
P_2O_5	.14	.35	.33	.24	.41	.61	.34	.56	.57	.44
CO_2	.19	.01	.01	.01	.01	.01	.01	.02	.02	.01
Total, in percent	99.94	99.64	99.58	99.76	99.76	99.55	99.79	99.76	99.38	99.84
Scandium	39.7	35.4	36.2	44.9	37.1	32.5	37.9	42.4	39.5	30.8
Chromium	244	63	54.9	123	40	49.2	227	77.4	67.9	30
Cobalt	53.2	47.7	46.1	50.5	39	36.4	35.4	50.1	48.4	34.4
Nickel	130	61	<30	95	<80	<60	68	76	83	<30
Zinc	89	130	140	110	140	150	100	160	170	140
Arsenic	<.5	1.4	<.9	<.6	1.8	1.2	<.6	<.6	<.7	<.7
Selenium	—	—	—	—	—	—	—	—	—	—

Table 4. Major and minor element geochemical analyses of Late Proterozoic metadiabase dikes.—Continued

[Sample locations with the prefix BR are found in Burton and others (1995), sample locations with the prefixes B, P, and HF are found in Southworth (1994, 1995) and Southworth and Brezinski (1996), and sample locations with the prefixes LN and RD are from J.S. Schindler (unpub. data). All analyses were performed at the U.S. Geological Survey, Reston, Va. Major element values were determined by X-ray spectroscopy by D.F. Siems and J.E Taggart; values for FeO, H_2O, and CO_2 were determined by X-ray spectroscopy by Hezekiah Smith, J.W. Marinenko, and J.R. Gillison. Minor element values were determined by Instrumental Neutron Activation Analysis by G.A. Wandless, P.A. Baedecker, J.S. Mee, and J.N. Grossman. Major element values are given in weight percent, and minor element values are given in parts per million. —, no data]

Dike type ➢	**Fine-grained**	**Fine-grained**	**Fine-grained**	**Fine-grained**	**Fine-grained**	**Fine-grained**	**Fine-grained**	**Fine-grained**	**Fine-grained**	**Fine-grained**
Sample no. ➢	**LN–252**	**LN–258**	**LN–261**	**LN–268**	**LN–270**	**LN–273**	**LN–276**	**LN–292A**	**LN–292B**	**LN–317**
Rubidium	14	24	46	32	40	41	77	13	45	54
Strontium	310	310	370	240	280	282	290	470	300	290
Zirconium	120	190	190	<50	230	260	190	210	220	260
Molybdenum	—	—	—	—	—	—	—	—	—	—
Antimony	.15	.24	<.11	<.1	<.08	<.16	<.08	<.11	<.12	<.09
Cesium	.25	.33	.4	.51	1.5	1.2	2.2	<.5	1.1	.99
Barium	120	180	220	170	270	280	180	75	270	290
Lanthanum	4.4	18	19	7.7	34	25	9.5	22	21	27
Cerium	10	42.4	42	18	49.5	53	22.2	51.4	47	57.1
Neodymium	9.3	25	26	12	41	31	17	33	29	32
Samarium	2.49	6.99	7.31	4.11	10.8	8.46	4.64	9.53	8.78	8.51
Europium	1.03	2.15	2.14	1.53	2.68	2.5	1.73	3.12	2.89	2.34
Terbium	.42	1.09	1.15	.8	1.58	1.31	.78	1.56	1.53	1.28
Ytterbium	1.9	2.8	3.5	2.8	4.98	3.6	2.6	5.28	4.74	3.84
Lutetium	.24	.39	.47	.39	.683	.49	.35	.715	.647	.525
Hafnium	1.5	4.82	4.97	2.5	6.15	6.3	2.79	6.3	5.82	6.4
Tantalum	.31	1.4	1.2	.51	1.4	1.67	.61	1.5	1.4	1.4
Gold	<5	<10	<2.8	<4	<2.1	<.3	<2.1	<.7	<.5	<5
Thorium	.28	1.7	1.5	.49	1.6	2.2	.48	1.2	1.3	2
Uranium	<.3	.4	.43	.26	.7	.69	.27	.4	.34	.59

Table 5. Major and minor element geochemical analyses of Late Proterozoic metabasalt of the Catoctin Formation.

[Sample locations with the prefix BR are found in Burton and others (1995), sample locations with the prefixes B, P, and HF are found in Southworth (1994, 1995) and Southworth and Brezinski (1996), and sample locations with the prefix LN are from J.S. Schindler (unpub. data). All analyses were performed at the U.S. Geological Survey, Reston, Va. Major element values were determined by X-ray spectroscopy by D.F. Siems and J.E. Taggart; values for FeO, H_2O, and CO_2 were determined by X-ray spectroscopy by Hezekiah Smith, J.W. Marinenko, and J.R. Gillison. Minor element values were determined by Instrumental Neutron Activation Analysis by G.A. Wandless, P.A. Baedecker, J.S. Mee, and J.N. Grossman. Major element values are given in weight percent, and minor element values are given in parts per million. —, no data]

Sample no. ➤	HF17	HF18	HF19	HF20	HF21	HF22	LN–31	LN–9C2	LN–9D2	LN–14	LN–15	LN–17	BR–807	BR–117
SiO_2	47.90	49.70	47.00	46.20	50.80	50.20	46.90	46.00	48.80	49.40	47.00	48.00	45.90	47.20
TiO_2	.97	3.10	2.23	3.17	2.53	.68	3.15	2.38	2.86	2.00	1.83	2.25	2.66	2.28
Al_2O_3	18.30	14.30	14.40	16.00	15.10	15.30	14.90	14.10	12.60	14.10	14.60	14.20	13.20	14.00
Fe_2O_3	10.42	9.13	4.52	8.09	9.42	2.45	14.09	4.90	7.44	5.64	4.46	3.95	5.38	5.08
FeO	4.40	5.20	7.10	6.50	4.40	7.70	.28	8.20	6.90	6.90	7.60	8.60	9.20	7.40
MnO	.28	.21	.34	.22	.20	.18	.22	.20	.21	.20	.20	.18	.24	.19
MgO	5.97	4.37	12.40	5.34	5.36	8.32	5.61	7.16	5.60	6.86	7.64	6.04	6.46	6.12
CaO	.87	3.92	2.28	6.25	6.64	11.50	8.28	10.90	9.24	7.95	10.00	10.90	11.20	10.80
Na_2O	5.99	1.92	2.60	4.02	1.22	1.86	3.66	2.35	3.47	4.23	2.96	2.62	2.13	1.88
K_2O	1.04	2.62	.04	.02	.02	.72	.65	.24	.24	.21	.09	.30	.28	.05
H_2O^+	3.20	3.50	5.90	3.50	3.40	.92	2.40	3.00	2.00	2.30	2.40	2.40	3.30	3.00
H_2O^-	.21	.12	.31	.12	.25	.48	.07	.14	.03	.05	.05	.34	.04	.11
P_2O_5	.09	.40	.25	.60	.28	.10	.34	.36	.26	.23	.23	.25	.39	.21
CO_2	.01	1.20	.19	.01	.01	.02	.02	.01	.01	.01	.44	.01	.01	1.00
Total, in percent	99.65	99.69	99.56	100.04	99.63	100.43	100.57	99.94	99.66	100.08	99.50	100.04	100.39	99.32
Scandium	33.7	28.1	37.5	24.8	34.9	42.1	28.6	36.4	35.7	37	35.8	36.3	34.9	42.5
Chromium	35.2	19.8	567	74.3	136	268	24	220	124	59.6	154	95.6	134	131
Cobalt	61.4	37.3	56.1	55.4	47.1	47.7	48.3	41.5	44.8	47.7	48.4	39.1	47.4	45
Nickel	134	<60	209	84	82	75	38	100	56	89	120	70	104	69
Zinc	199	81	132	155	131	92	114	110	120	120	110	120	71	126
Arsenic	<1	<1	<2	<1	1.04	2	<1.3	1.0	< 1.10	<.8	< .700	<1.00	<1	<.6
Selenium	—	—	—	—	3	—	—	—	—	—	—	—	<2	<2
Rubidium	27.4	52.3	<6	<6	6	38.6	20	17	< 8.00	6.5	< 5.00	15	<7	11.2

Table 5. Major and minor element geochemical analyses of Late Proterozoic metabasalt of the Catoctin Formation.—Continued

[Sample locations with the prefix BR are found in Burton and others (1995), sample locations with the prefixes B, P, and HF are found in Southworth (1994, 1995) and Southworth and Brezinski (1996), and sample locations with the prefix LN are from J.S. Schindler (unpub. data). All analyses were performed at the U.S. Geological Survey, Reston, Va. Major element values were determined by X-ray spectroscopy by D.F. Siems and J.E. Taggart; values for FeO, H_2O, and CO_2 were determined by X-ray spectroscopy by Hezekiah Smith, J.W. Marinenko, and J.R. Gillison. Minor element values were determined by Instrumental Neutron Activation Analysis by G.A. Wandless, P.A. Baedecker, J.S. Mee, and J.N. Grossman. Major element values are given in weight percent, and minor element values are given in parts per million. —, no data]

Sample no. ➢	HF17	HF18	HF19	HF20	HF21	HF22	LN–31	LN–9C2	LN–9D2	LN–14	LN–15	LN–17	BR–807	BR–117
Strontium	<140	130	<120	700	530	160	470	360	300	110	280	410	280	291
Zirconium	160	300	220	240	190	<120	130	270	200	190	<200	240	200	200
Molybdenum	3	<7	<7	<4	5	<10	—	—	—	—	—	—	<4	<6
Antimony	<.09	.14	.13	<.09	.14	<.1	<.1	<.100	< .110	<.12	.20	.15	.16	<.1
Cesium	.43	.71	<.2	<.2	.2	.45	.23	<.260	<.270	<.22	<.250	<.260	<.2	<.3
Barium	209	476	<40	<100	40	134	200	130	83	100	79	99	<120	88
Lanthanum	4.61	37.9	21.7	25.8	16.6	4.9	30.7	10.6	12.8	14.4	7.8	15.7	12.5	12.2
Cerium	10.1	73.7	41.2	53.8	36.6	10.7	61.4	25	30.6	31.3	18	33.1	28.5	28
Neodymium	6.5	35.9	22.7	30.2	23.3	6.6	30	15	20	19	14	20	18.3	20
Samarium	2.33	8.58	5.91	7.73	6.59	1.95	6.96	4.84	6.23	5.38	3.91	5.78	4.94	5.96
Europium	.985	2.5	1.76	2.53	2.04	.692	2.17	1.90	2.00	1.67	1.5	1.76	1.64	2.14
Terbium	.67	1.31	.92	1.17	1.09	.53	.93	.87	1.10	.873	.74	1.01	.82	1.03
Ytterbium	2.88	3.17	2.35	2.93	3.18	2.06	2.2	2.6	2.88	2.66	2.5	2.88	2.21	3.42
Lutetium	.42	.439	.327	.491	.435	.3	.32	.39	.404	.369	.34	.401	.294	.494
Hafnium	1.1	6.16	3.69	4.62	4.72	1.36	4.58	3.0	4.41	3.73	2.4	4.18	3.25	3.67
Tantalum	.2	2.68	1.14	1.92	1.02	.231	2.38	.62	1.08	.87	.48	1.02	1.03	.73
Gold	16.6	<8	<7	<6	<1	<10	<2	< 1.50	8.8	<2.2	< 1.60	<1.60	<9	11.6
Thorium	.26	4.16	2.5	2.03	1.22	1.09	3.68	.41	1.3	1.3	.39	1.5	1.15	.75
Uranium	<.4	1.06	<.4	.57	.48	.44	.62	<.310	.41	.26	<.290	.53	.27	<.4

Table 5. Major and minor element geochemical analyses of Late Proterozoic metabasalt of the Catoctin Formation.—Continued

[Sample locations with the prefix BR are found in Burton and others (1995), sample locations with the prefixes B, P, and HF are found in Southworth (1994, 1995) and Southworth and Brezinski (1996), and sample locations with the prefix LN are from J.S. Schindler (unpub. data). All analyses were performed at the U.S. Geological Survey, Reston, Va. Major element values were determined by X-ray spectroscopy by D.F. Siems and J.E. Taggart; values for FeO, H_2O, and CO_2 were determined by X-ray spectroscopy by Hezekiah Smith, J.W. Marinenko, and J.R. Gillison. Minor element values were determined by Instrumental Neutron Activation Analysis by G.A. Wandless, P.A. Baedecker, J.S. Mee, and J.N. Grossman. Major element values are given in weight percent, and minor element values are given in parts per million. —, no data]

Sample no. ➤	B3	B4	B5	B6	B7	B8	P8	P9	P10	P11	P12	P13
SiO_2	46.10	51.60	59.60	47.90	46.00	46.90	46.40	48.10	49.00	48.00	48.70	50.00
TiO_2	2.83	2.46	2.33	2.61	3.69	1.92	1.47	1.76	2.54	1.56	3.06	.13
Al_2O_3	17.30	12.20	10.90	13.60	13.70	14.40	13.30	15.60	12.90	13.10	12.90	13.80
Fe_2O_3	9.46	4.51	6.81	3.68	3.59	4.17	5.87	7.99	6.96	2.70	5.53	7.22
FeO	4.90	8.10	3.60	9.30	7.40	9.40	4.80	4.60	6.80	8.20	9.80	6.20
MnO	.16	.21	.20	.26	.37	.24	.18	.14	.20	.18	.30	.23
MgO	4.23	6.42	3.87	7.12	3.67	8.84	9.92	6.21	6.63	11.10	5.03	6.95
CaO	6.23	7.92	9.92	7.72	9.33	4.89	11.60	7.77	9.27	7.03	5.27	8.18
Na_2O	5.00	3.81	<.15	3.45	4.31	3.99	2.04	4.59	2.55	2.12	3.39	<.15
K_2O	.51	.07	<.02	.42	.03	.30	.45	.17	.19	1.57	.09	<.02
H_2O^+	2.80	2.70	2.70	3.50	3.20	4.50	2.70	2.10	3.00	4.20	4.00	4.70
H_2O^-	.23	.11	.12	.34	.13	.23	.17	.22	.13	.24	.14	2.41
P_2O_5	.37	.22	.22	.22	1.03	.20	.14	.18	.22	.18	.51	.28
CO_2	.01	.02	.02	<.01	3.90	<.01	<.01	<.01	.02	.02	1.60	.02
Total, in percent	100.13	100.35	100.46	100.13	100.35	99.99	99.05	99.44	100.41	100.20	100.32	100.29
Scandium	24.2	38.4	23.8	32	28.2	37.6	37.3	31.3	37.9	30.2	30	36.6
Chromium	63.3	95	32.5	71.9	8.6	124	781	115	92	693	12.2	78.1
Cobalt	55.1	48.8	43.9	38.5	36.5	59.2	53.1	41.3	47.4	52.1	36.1	44.8
Nickel	77	75	53	64	<60	102	402	85	89	188	<23	50
Zinc	120	119	119	137	220	185	76.6	71	118	97	184	103
Arsenic	<1	<.8	.69	1.7	<2	<1	2.8	2.8	<.7	<.5	3.5	.73
Selenium	—	<2	<2	<.6	<3	<2	—	—	<2	<.3	<3	<3
Rubidium	20.8	<5	<4	16.8	<5	9.4	11	<5	11	27	6.6	<5

Table 5. Major and minor element geochemical analyses of Late Proterozoic metabasalt of the Catoctin Formation.—Continued

[Sample locations with the prefix BR are found in Burton and others (1995), sample locations with the prefixes B, P, and HF are found in Southworth (1994, 1995) and Southworth and Brezinski (1996), and sample locations with the prefix LN are from J.S. Schindler (unpub. data). All analyses were performed at the U.S. Geological Survey, Reston, Va. Major element values were determined by X-ray spectroscopy by D.F. Siems and J.E. Taggart; values for FeO, H_2O, and CO_2 were determined by X-ray spectroscopy by Hezekiah Smith, J.W. Marinenko, and J.R. Gillison. Minor element values were determined by Instrumental Neutron Activation Analysis by G.A. Wandless, P.A. Baedecker, J.S. Mee, and J.N. Grossman. Major element values are given in weight percent, and minor element values are given in parts per million. —, no data]

Sample no. ➢	**B3**	**B4**	**B5**	**B6**	**B7**	**B8**	**P8**	**P9**	**P10**	**P11**	**P12**	**P13**
Strontium	500	<90	1,050	440	<190	<170	590	480	230	134	<150	270
Zirconium	280	210	180	164	190	186	140	170	100	180	220	180
Molybdenum	<6	<6	<4	<6	<5	<5	<7	<6	<5	<5	<6	<4
Antimony	.11	<.1	.096	<.3	.12	<.1	<.09	<.2	<.1	<.09	.33	.091
Cesium	.24	<.3	<.2	.27	<.2	<.5	<.2	<.2	<.3	.38	.31	<.3
Barium	120	<30	<28	142	<31	137	110	63	53	505	61	<70
Lanthanum	23.2	11.9	12.4	13	33.9	14.3	6.07	6.63	10.7	10.08	25.6	16.9
Cerium	48.4	27.1	29.1	27.5	74.3	33.9	15.2	17.9	24.7	21.8	55.3	34.2
Neodymium	25.1	17.9	19.7	17.3	42.4	18.8	10.5	11.2	16.1	12.8	34.4	20.8
Samarium	6.6	5.32	5.66	4.77	10.27	5.17	3.33	3.32	5.37	3.72	9.02	6.09
Europium	2.17	1.36	1.83	1.51	4.52	1.41	1.15	1.4	1.76	1.13	2.52	1.88
Terbium	.97	.97	.926	.786	1.34	.89	.65	.634	.97	.64	1.37	1.01
Ytterbium	2.58	2.7	2.25	2.21	3.34	2.75	2.04	1.98	2.72	2.27	4.18	2.8
Lutetium	.354	.394	.331	.327	.462	.399	.298	.276	.392	.332	.592	.397
Hafnium	4.29	3.58	3.8	3.28	5.5	3.7	2.12	2.25	3.65	2.47	6.37	4.15
Tantalum	1.93	1.01	.94	.87	2.24	.92	.384	.608	.75	.564	1.37	.96
Gold	<4	<7	<5	<4	<3	<11	<2	<7	<2	<3	—	<4
Thorium	2.33	1.23	1.14	.98	3.42	1.85	.47	.55	.91	.83	1.98	1.21
Uranium	.76	.25	.25	.39	.7	.56	<.4	<.3	.18	<.3	.6	.34

basins. Spectacular outcrops of metaconglomerate can be seen along the bluffs of Goose Creek east of Leithtown (Kline and others, 1991), in which pebbles and cobbles are predominantly granite gneiss derived from nearby sources. Crossbedded meta-arkose can be seen along Goose Creek just east of Carters Bridge, and metasiltstone and metamudstone are well exposed along Little River, south of Dover. To the south, strata of the Fauquier Formation dramatically increase in thickness, and the relation of these rocks with the Lynchburg Group are discussed by Kline and others (1991), Wehr (1985), Kasselas (1993), and Rader and Evans (1993).

Swift Run Formation

Rocks of the Swift Run Formation (Stose and Stose, 1946; King, 1950) can be divided into a coarser grained, psammitic lower part (Zss) and a finer grained, phyllitic upper part (Zsp). The lower part consists of metagraywacke, quartz-sericite schist, metasandstone, quartzite, and meta-arkose. The upper part consists of marble, slate, and phyllite. Bodies of calcitic and dolomitic marble (Zsm) are mapped separately both near the base and near the top of the section. The thickness of the Swift Run Formation varies from zero in places to more than 700 ft, and the strata are discontinuous over short distances.

The clastic rocks fine upward, and the crossbedding suggests that these rocks are of fluvial origin. The marble horizons may be shallow water lakes and ponds (McDowell and Milton, 1992) and (or) intertidal to subtidal marine embayments (Kline and others, 1991). The basal metasandstone west of Loudoun Valley Church contains quartz pebbles and cobbles, and lithic clasts of phyllite and ferruginous sandstone (Southworth, 1991). Quartz-sericite schist preserved in downfolded inliers can be seen near Elvan and the confluence of Dutchman Creek and the Potomac River (Southworth, 1991). Impressive outcrops of marble, slate, and phyllite are found west of Silcott Spring (Southworth, 1994). Basal conglomerate and pebbly quartzite (Zss) and overlying sericite phyllite (Zsp) and marble (Zsm) are exposed north of Paeonian Springs (Burton and others, 1995). Some of the phyllite may be tuffaceous deposits that preceded Catoctin volcanism (Burton and others, 1995). Metabasalt and rip-up conglomerate of metabasalt found in quartz-sericite schist (Zss) (Southworth, 1995) suggests that some of the basal rocks of the Swift Run Formation on the west limb of the Blue Ridge anticlinorium were deposited after the beginning of Catoctin volcanism.

Catoctin Formation

The Catoctin Formation (Keith, 1894) is characterized by dark-green to bluish-gray, fine-grained to aphanitic metabasalt (Zc) that varies texturally from massive, locally amygdaloidal greenstone to well-foliated greenschist. Individual flows are difficult to recognize due to strong Paleozoic deformation, metamorphism, and poor exposure. Metabasalt breccia (Zcb) is found near the base of the Catoctin north and southwest of Aldie. Epidosite, a fine-grained, massive, apple-green rock consisting of epidote and quartz occurs as discontinuous layers or boudins as much as a few feet in length.

The Catoctin Formation contains interbeds of gray- to buff-weathering marble (Zcm), white metarhyolite and quartz-sericite phyllite interpreted as felsic metatuff (Zcr), gray to buff feldspathic metasandstone (Zcs), and gray quartz-graphite-muscovite phyllite (Zcp). Marble occurs both as a continuous layer at the base of the Catoctin and as a discontinuous horizon at or near the base. The marble is best seen along Goose Creek, west of Oatlands, in abandoned pits where it was quarried for agricultural lime and ornamental stone (Kline and others, 1991). North of Taylorstown, marble is found as a very thin 3- to 9-ft-thick horizon about 66 ft above the base of the Catoctin.

The felsic metatuff (Zcr) lithologically resembles the tuffaceous(?) phyllite of the Swift Run Formation (Zsp) (Burton and others, 1995). Felsic metatuff and metarhyolite (Zcr) occur in the lower, middle, and upper parts of the Catoctin Formation, stratigraphically above and below muscovite phyllite (Zcp) on the west limbs of the anticlinorium (Southworth, 1991, 1994, 1995). On the east limb, quartz-graphite-muscovite phyllite (Zcp) occurs only in the upper part of the Catoctin, and thin, 3- to 7-ft-thick discontinuous lenses of crossbedded arkosic metasandstone (Zcs) occur in the middle part of the formation (Burton and others, 1995).

The Catoctin Formation shows considerable variation in apparent thickness, ranging from about 2,500 to 5,000 ft on the east limb of the anticlinorium and as much as 1,640 ft on the west limbs. The wide map pattern of the Catoctin Formation on the east limb could be due to unrecognized Paleozoic folds or Mesozoic normal faults. The total absence of Catoctin Formation on Purcell Knob (Blue Ridge) indicates that at least some of the variation reflects true thickening and thinning of the metabasalt and intercalated units (Southworth, 1991).

Age of the Catoctin Formation

An Rb/Sr age of 570±36 Ma was obtained from metabasalt of the Catoctin Formation by Badger and Sinha (1988) in central Virginia. A metarhyolite tuff (Zcr) near Bluemont (Southworth, 1994) yielded an approximate U-Pb age of 600 Ma (table 3, sample no. 5), and metarhyolite from South Mountain, Pa., yielded a U-Pb age of 597±18 Ma. Felsic metatuff (Zcr) in the Catoctin Formation near its base along the Potomac River north of Taylorstown is the nearest extrusive equivalent to a 571.5±5-Ma metarhyolite dike (Aleinikoff and others, 1995) in the nearby basement core and suggests that the upper part of the Catoctin Formation is younger than 570 Ma (Burton and others, 1995).

Paleozoic Rocks of the Blue Ridge Anticlinorium

The Chilhowee Group (Safford, 1856) in northern Virginia consists of the Loudoun Formation, Weverton Formation, Harpers Formation, and Antietam Quartzite (Keith, 1894). The contact between the Chilhowee Group and the underlying Catoctin Formation has been interpreted to be either conformable (Nickelsen, 1956) or unconformable (King, 1950; Reed, 1955); both relations are found in Loudoun County. Rocks of the Chilhowee Group are interpreted to be a marine transgressive sequence exhibiting a depositional transition from rift to passive continental margin that is marked by the conformably overlying carbonate rocks.

Loudoun Formation

The Loudoun Formation (Keith, 1894; Whitaker, 1955; Nickelsen, 1956) is a thin, discontinuous unit of predominantly phyllite and minor conglomerate that occurs locally between the Catoctin and Weverton Formations. Near the Potomac River on Catoctin Mountain, black phyllite interbedded with pebbly metasandstone occurs above interlayered dark-bluish-gray graphite-muscovite phyllite and greenstone of the Catoctin Formation (Burton and others, 1995). Here, the black phyllite is in sharp contact with the white, massive, vitreous quartzite of the overlying Weverton Formation.

The Loudoun Formation on Blue Ridge consists of a lower phyllite member (€l) and an upper coarse quartz-pebble conglomerate member (€lc). The phyllite is similar to phyllites in the Catoctin Formation (Stose and Stose, 1946; King, 1950; Reed, 1955; Toewe, 1966; Gathright and Nystrom, 1974; Southworth, 1991), and the conglomerate is locally interbedded with quartzite (Southworth, 1991). The base of the phyllite is gradational with the underlying Catoctin Formation and is interbedded with greenstone that contains micaceous blebs (amygdules?) and tuffaceous clasts (Southworth and Brezinski, 1996). The conglomerate is a lensoid, discontinuous, coarse quartz-pebble conglomerate that is interpreted to be channel fill cut into the underlying phyllite (Southworth, 1991). The conglomerate is arkosic and contains coarse-grained and cross-stratified beds. Cross-stratified quartzite occurs between the conglomerate and phyllite in several places and can be seen north of Purcell Knob, west of Neersville (Southworth and Brezinski, 1996). Rip-up clasts of phyllite and red jasper in the conglomerate suggest a period of erosion between deposition of the two members.

Weverton Formation

The Weverton Formation (Keith, 1894) is divided into three informal members (Nickelsen, 1956) on the west limbs of the Blue Ridge anticlinorium and has not been subdivided on the east limb. The lower member of the Weverton Formation (€wl) is mostly a light-gray, massive, thick-bedded vitreous quartzite that is interbedded with minor metagraywacke and metasiltstone. The middle member (€wm) is a greenish-gray, granular quartzite interbedded with metasiltstone. The upper member (€wu) is a dark-gray to dusky "gun-metal" blue, poorly sorted, locally crossbedded quartzite and quartz-pebble conglomerate interbedded with metasiltstone. The Weverton Formation on the east limb (€w) is a light-gray, massive to thick-bedded vitreous quartzite with minor phyllitic interbeds that is lithologically correlative with the lower member (€wl). Where present, the lower member grades upward from conglomerate of the Loudoun Formation. Elsewhere, the lower member quartzite appears to be in sharp contact with phyllite of the Loudoun Formation or metabasalt of the Catoctin Formation. On Short Hill Mountain, the upper member grades into the finer grained metasiltstone of the overlying Harpers Formation. On Catoctin Mountain vitreous quartzite of the Weverton Formation (€w) grades into quartzose phyllite of the Harpers Formation over a few feet.

Rocks of the Weverton Formation show considerable variation in lithology and thickness across the Blue Ridge anticlinorium. More than 660 ft of Weverton Formation is present on Blue Ridge (Nickelsen, 1956; Southworth, 1991; McDowell and Milton, 1992) and on Short Hill Mountain (Nickelsen, 1956; Southworth, 1991, 1995) but only 115 ft is found on Catoctin Mountain (Whitaker, 1955; Burton and others, 1995). On Catoctin Mountain, the Weverton Formation thickens northward to 427 ft in Frederick County, Md. (Whitaker, 1955), and it thickens southward along Bull Run Mountain to 1,247 ft at Thoroughfare Gap in Fauquier County, Va. (P.T. Lyttle, oral commun., 1993).

The Weverton Formation is interpreted to result from alluvial sedimentation (Schwab, 1986), and paleocurrent directions suggest a source from the west (Whitaker, 1955). These rocks reflect a change from a volcanic to a predominantly fluvial environment (Nickelsen, 1956). Individually, the lower, middle, and upper members are fining-upward sequences, but the upper member is coarser and more poorly sorted. These rocks of the upper member can be seen north of the gap on Short Hill Mountain at Hillsboro (Southworth, 1995) and along the Appalachian National Scenic Trail on Blue Ridge (McDowell and Milton, 1992).

Harpers Formation

The Harpers Formation (€h) (Keith, 1894) is predominantly siltstone that has been metamorphosed into quartz-laminated metasiltstone and biotite-chlorite-muscovite-quartz phyllite. Primary sedimentary structures are obscure due to recrystallization and pervasive cleavage. On Catoctin Mountain, quartzite of the Weverton Formation (€w) grades upward into interbedded metasiltstone and phyllite of the Harpers Formation. The best exposures of the Harpers Formation in Loudoun County are along the bluffs of the Potomac River on Short Hill Mountain (Southworth, 1991).

Antietam Quartzite

The Antietam Quartzite (€a) (Keith, 1894) is a poorly exposed, generally massive meta-arkose that is mapped mostly by its ledge-forming topographic expression and float from Stumptown to Furnace Mountain. The Antietam Quartzite is gradational and conformable with the underlying phyllite of the Harpers Formation. Near its upper contact with carbonaceous phyllite (€cp) or the Tomstown Formation (€t), the Antietam

Quartzite contains concentrations of limonite that were mined for iron ore in the vicinity of Furnace Mountain in the 19th century (Holden, 1907). The Antietam Quartzite was correlated with the Araby Formation by Reinhardt (1977).

Carbonaceous Phyllite

Overlying the Antietam Quartzite locally is a dark-gray, very fine grained carbonaceous phyllite (Ꞓcp) that is rarely exposed but produces a distinctive, light-gray, ashy-looking soil. Fine-bedding laminae in the metamudstone are seen in road banks north of Stumptown. The carbonaceous rock is in the same stratigraphic position as the Tomstown Formation and apparently interfingers with it. Carbonaceous phyllite is lithologically similar to a black shale called the Cash Smith Formation by Edwards (1988) that occurs between the Araby Formation and the Frederick Limestone to the northeast (Jonas and Stose, 1938; Stose and Stose, 1946).

Tomstown Formation

Buff-weathering, white to bluish-gray, medium-grained dolostone of the Tomstown Formation (Stose, 1906) is exposed in the vicinity of Furnace Mountain. The dolostone apparently conformably overlies the Antietam Quartzite. It interfingers with and is stratigraphically equivalent to a carbonaceous phyllite. The dolostone is correlative to the dolomite of the Bolivar Heights Member of the Tomstown Formation (Brezinski, 1992), as mapped on the west limb of the Blue Ridge anticlinorium in Maryland.

Frederick Limestone

Gray, thin-bedded limestone of the Rocky Springs Station Member of the Frederick Limestone (Reinhardt, 1977) is exposed east of Furnace Mountain where it overlies dolostone of the Tomstown Formation. This contact may be an unconformity or a major fault because the Tomstown Formation is of Early Cambrian age (Bassler, 1919) and the Frederick Formation is of Late Cambrian age (Reinhardt, 1977). Whitaker (1955) recognized this and other anomalous stratigraphic relations of the Harpers Formation, Antietam Quartzite, Tomstown Formation, and Frederick Formation to the north. He suggested faulting, facies changes, and (or) one or more unconformities to account for these relations. Elsewhere in this region, rocks of the Tomstown Formation and Frederick Limestone are separated by Mesozoic normal faults (Jonas and Stose, 1938).

Paleozoic Structure

The Mesoproterozoic and Late Proterozoic and lower Paleozoic rocks of the Blue Ridge province were deformed and metamorphosed in the late Paleozoic Alleghanian orogeny to produce the Blue Ridge anticlinorium. The anticlinorium is a broad, highly asymmetrical west-verging and gently north-plunging fold with a generally homoclinal, gently dipping east limb and more complexly deformed and tightly folded, commonly overturned, west limbs. The core of the anticlinorium contains Mesoproterozoic gneisses and Late Proterozoic plutons and dikes, and the limbs are mantled by a cover sequence of Late Proterozoic to Lower Cambrian metasedimentary and metavolcanic rocks. The west limb of the Blue Ridge anticlinorium is repeated by the Short Hill fault, an early Paleozoic normal fault that was contractionally reactivated as a thrust fault and folded during the formation of the anticlinorium. Alleghanian deformation was accompanied by a main fold phase (F_1) and regional, penetrative, axial planar cleavage (S_1); a later, minor fold phase (F_2) and local crenulation cleavage (S_2); and extensive recrystallization and development of metamorphic textures under lower greenschist-facies conditions.

F_1 Folds and S_1 Cleavage

The Blue Ridge anticlinorium is a large west-verging F_1 fold with an east limb that underlies Catoctin Mountain and fault-repeated west limbs that underlie Blue Ridge and Short Hill Mountain. Map-scale parasitic folds include the Purcell Knob folds on Blue Ridge, the Hillsboro syncline that underlies Short Hill Mountain and Black Oak Ridge, two synclines of the Swift Run Formation east of Short Hill Mountain, and the Furnace Mountain syncline on Catoctin Mountain. Second- and third-order, tight recumbent folds of the Weverton Formation that verge up the west limb of the anticlinorium can be seen along the Potomac River gorge northwest of Loudoun Heights (Southworth and Brezinski, 1996).

Approximately axial planar to the Blue Ridge anticlinorium and probably coeval with its formation is a regional penetrative northeast-striking, southeast-dipping S_1 cleavage (South Mountain cleavage of Cloos (1951) and Mitra and Elliott (1980)) that overprints Mesoproterozoic metamorphic fabrics in the gneisses, primary igneous textures in the Late Proterozoic dikes, and primary volcanic and sedimentary textures in the cover-sequence rocks. S_1 ranges from slaty to schistose in texture depending on the nature of the host material. Poles to S_1 show a tight cluster indicative of a regionally uniform, southeast-dipping penetrative fabric (fig. 3*F–I*, on map sheet).

F_2 Folds and S_2 Cleavage

Late deformation produced locally developed, open to tight folds (F_2) that are accompanied by an axial planar crenulation cleavage, as well as a regional spaced cleavage (S_2). This deformation may have been a continuum of the earlier, main phase of deformation that produced the F_1 and S_1 structures (Nickelsen, 1956). On the limbs of the Blue Ridge anticlinorium, F_2 folds refold F_1 folds and S_1 cleavage; on the west limb, examples can be seen on the Blue Ridge from Wilson Gap to north of Purcell Knob (Nickelsen, 1956; Southworth, 1991) and on the east limb, examples can be seen on Catoctin Mountain (Burton and others, 1995). Lateral bends and cross folds are later superimposed on folds near Trapp and along Short Hill Mountain. S_2 cleavage is not penetrative, did not involve extensive recrystallization, and is mostly a pressure solution cleavage. S_2 has about the same strike as S_1 but a slightly steeper dip (fig. 3*K*, on map sheet) or narrow range of dips (fig. 3*J*, on map sheet). The summed effect of F_1 and F_2 folds are illustrated by poles to bedding in quartzite of the Weverton Formation on Blue Ridge and Short Hill Mountain (fig. 3*L* and *M*, on map sheet). The tight cluster of data on Short Hill Mountain reflects the southeast-dipping homoclinal limbs of the isoclinal Hillsboro syncline (Southworth, 2005). The girdle of data on Blue Ridge indicates the abundance of westward-inclined, shallow-northeast-plunging parasitic folds.

Faults

Faults were mapped on the basis of stratigraphic truncation and omission in the cover sequence and shear foliation in the basement gneiss. East- and north-trending faults near Mountville are interpreted to be Late Proterozoic normal faults that were active during deposition of rocks of the Fauquier Formation (Kline and others, 1991). A similar east-trending normal fault marks the southern termination of the Swift Run Formation on the east limb of the anticlinorium.

The Short Hill fault can be traced for over 37 mi from a shear zone in basement gneiss in Fauquier County, Va., into Washington County, Md., where rocks of the Tomstown Formation overlie rocks of the Catoctin and Weverton Formations (Southworth, 2005). The Short Hill fault is interpreted to be an early Paleozoic normal fault (post-Tomstown Formation, but possibly post-Elbrook Formation (Brezinski, 1992)) that was contractionally reactivated and folded with the Blue Ridge anticlinorium in the Alleghanian orogeny (Southworth, 2005).

Strike-slip faults with minor displacement offset strata on Blue Ridge west of Round Hill (McDowell and Milton, 1992). The White Rock thrust fault (Southworth, 1991) is an intraformational bedding-parallel detachment in the middle member of the Weverton Formation on Short Hill Mountain. It is marked by blocks of quartzite as long as 3 ft that float in a matrix of foliated vein quartz that constitutes as much as 80 percent of outcrops.

The Mesoproterozoic basement of the Blue Ridge anticlinorium contains zones of mylonite and phyllonite that cut Mesoproterozoic structures and juxtapose map units. Some of these, such as the zone of mylonitic foliation east of the Short Hill fault south of Black Oak Ridge (Southworth, 1994), were previously mapped as metasedimentary rocks by Jonas (1928) and Parker (1968). The shear zones contain a lower greenschist-facies mineralogy that is consistent with the grade of Paleozoic metamorphism and are thought to have formed contemporaneously with contractional deformation in the Paleozoic. The Dutchman Creek shear zone (Southworth, 1991) is 0.62 mi wide and contains internal mylonite zones ranging from 1 to 6 ft thick. The fault zone thrusts biotite granite gneiss (Ybg) westward onto garnetiferous leucocratic metagranite (Ygt), and the mylonites have sense of shear indicators that consistently show east over west motion. To the east of Dutchman Creek, anastomosing shear zones in basement gneiss have kinematic indicators that record both east-side-up and east-side-down sense of movement (Burton and others, 1995). The field aspect and mineralogy of the normal-sense shear zones are identical to those that record reverse sense, and they are considered to be the same age.

Paleozoic Metamorphism

Paleozoic deformation was accompanied by recrystallization under lower greenschist-facies metamorphic conditions. Formation of S_1 was accompanied by the growth of fine-grained secondary muscovite, chlorite, biotite, epidote, actinolite, and accessory minerals. Plagioclase in all rocks typically has cloudy overgrowths of sericite and saussurite and is now albite compositionally. Quartz grains have undulatory extinction or have recrystallized into a fine-grained mosaic. This metamorphism produced widespread biotite in pelitic rocks of the east limb but no garnet, indicating that metamorphic grade did not reach upper greenschist facies. Recrystallization in the Mesoproterozoic gneisses produced low-grade mineral assemblages that contrast sharply with the original Mesoproterozoic high-grade assemblages. In the granitic rocks, muscovite, chlorite, epidote, and secondary greenish biotite grew at the expense of feldspar and primary brown biotite. Garnet is largely chloritized, and mafic minerals are uralitized or extensively altered to actinolite and chlorite. The greenstone dikes and the metabasalts of the Catoctin Formation have typical mafic greenschist-facies mineral assemblages of actinolite, chlorite, and epidote. Muscovite, derived from feldspar, is also common, and minor greenish-brown biotite and pale-brown stilpnomelane is locally present. In pelitic rocks such as phyllite of the Harpers Formation on the east limb, muscovite, biotite, and chlorite are well developed and define the S_1 cleavage.

$^{40}Ar/^{39}Ar$ Dating of Metamorphic Fabric

Muscovite and phlogopite that define the dominant cleavage in several cover-sequence lithologies have been analyzed by the $^{40}Ar/^{39}Ar$ age-spectrum technique in order to determine the age of the foliation and the timing of Paleozoic deformation and metamorphism. The rock units sampled include strongly cleaved quartzite of the Weverton Formation (Ꞓw) and phlogopitic marble (Zcm) of the Catoctin Formation (table 3, sample nos. (1) and (2), respectively). With one exception, the penetrative micaceous foliation in these rocks is first-generation (S_1) and therefore thought to be coeval with formation of the Blue Ridge anticlinorium.

Most of these samples yield complex spectra that do not have plateaus and do not yield precise estimates of the timing of muscovite growth (Burton and others, 1992b; Kunk and others, 1993). The data suggest that the muscovite is of multiple generations, although petrographic examination of these rocks shows only one well-developed generation of cleavage-defining mica. There was apparently an early episode of minor mica growth followed by the main cleavage-producing event, with the latter occurring at temperatures below the argon closure temperature for muscovite (~350 °C) (Kunk and others, 1993). These data suggest a late Paleozoic (Alleghanian) age (350–300 Ma) for the development of the regional cleavage of the Blue Ridge anticlinorium, and they seem to rule out a pervasive early Paleozoic (Taconian) metamorphic event (Burton and others, 1992b).

Piedmont Province

Potomac Terrane

A small area of quartz-rich schist (€Zms) and graded beds of metagraywacke (€Zmg) of the Mather Gorge Formation (Drake and Froelich, 1986) is exposed along the Potomac River in the extreme northeastern part of the county. The metagraywacke beds grade up into laminated beds and then schist. These metasedimentary rocks originated as turbidites that were deposited in a large submarine fan of unknown age (Drake and Morgan, 1981). These structurally complex, chlorite-grade rocks increase eastward to sillimanite-grade rocks produced by a Barrovian metamorphic event. The timing of the metamorphism and deformation is uncertain. It is interpreted, however, to be related to the accretion of these rocks onto the rise-slope strata of the Westminster terrane along the Pleasant Grove fault during closure of the Iapetus Ocean in the Ordovician Taconian orogeny (Drake and others, 1989). Rocks of the Westminster terrane are thrust on rocks of Laurentia along the Martic fault (fig. 1) (Southworth, 1998), but these rocks are covered by the Culpeper basin in Loudoun County.

Mesozoic Rocks of the Lower Culpeper Group

The Culpeper Group (Lee, 1979, 1980) of the Newark Supergroup (Froelich and Olsen, 1984) is divided informally into a lower part and an upper part. The lower part of the Culpeper Group includes the mainly Upper Triassic sequence of continental sedimentary rocks that consists of the Manassas Sandstone, the Balls Bluff Siltstone, and the Catharpin Creek Formation.

Manassas Sandstone

The Manassas Sandstone (Lee, 1977, 1979) is divided into the Reston Member (Lee, 1977; Drake and Lee, 1989) and the Poolesville Member (Lee and Froelich, 1989).

Reston Member

The Reston Member (₸mr) is the basal conglomerate that is faulted against and unconformably overlies rocks of the Mather Gorge Formation in the extreme eastern part of the county. The conglomerate is composed of cobbles and pebbles of micaceous quartz, metagraywacke, and schist in a poorly sorted arkosic sandstone matrix. The lensoid, discontinuous conglomerate is derived from rocks of the Mather Gorge Formation by unconformable onlap and (or) erosion of normal fault scarps.

Poolesville Member

The Poolesville Member (₸mp) is an arkosic and micaceous sandstone. Regionally, the Poolesville Member is an upward-fining sequence but pebbly sandstone and siltstone intertongue locally. These rocks are gradational to the underlying Reston Member and the overlying Balls Bluff Siltstone. Rocks of the Poolesville Member are found east of Sugarland Run, but the best exposures are along the bluffs of the Potomac River northeast of Lucketts. In Fairfax County, the Poolesville Member of the Manassas Sandstone has yielded footprints of the crocodilomorphs *Chirotherium lulli* and *Brachychirotherium parvum*, as well as a footprint of a small birdlike animal called *Plesiornis pilulatus* (Weems and Kimmel, 1993).

Balls Bluff Siltstone

The Balls Bluff Siltstone (Lee, 1977, 1979) is divided into the Leesburg Member (Lee and Froelich, 1989), the fluvial and deltaic sandstone and siltstone member (informal) (J.P. Smoot, A.J. Froelich, and R.E. Weems, unpub. data), and the lacustrine shale and siltstone member (informal) (J.P. Smoot, A.J. Froelich, and R.E. Weems, unpub. data).

Leesburg Member

The Leesburg Member (₸bl) is a conspicuous carbonate conglomerate composed of subangular to subrounded boulders, cobbles, and pebbles of limestone and dolomite in a reddish-brown sandy siltstone matrix. Large, isolated outcrops are well exposed along the Route 15 corridor north of Leesburg. The source of the carbonate clasts includes the dolomite and limestone of the Tomstown Formation and Frederick Limestone that are presently restricted to Furnace Mountain and north of the Potomac River in Frederick County, Md. The conglomerate intertongues with the sandstone and siltstone of the other members and forms a complex map pattern. The conglomerate is interpreted to be debris-flow deposits on alluvial fans (Smoot, 1989). The conglomerate was quarried as Potomac marble and was used for the columns in Statuary Hall of the Capitol Building in Washington, D.C.

Fluvial and Deltaic Sandstone and Siltstone Member

The fluvial and deltaic sandstone and siltstone member (informal) (₸bs) is predominantly feldspathic, silty sandstone interbedded with clayey and sandy siltstone in cyclic sequences as much as 10 ft thick. This unit is gradational with the underlying Poolesville Member of the Manassas Sandstone and intertongues laterally with carbonate conglomerate of the Leesburg

Member and the lacustrine shale and siltstone member. These rocks are conformably overlain by rocks of the Catharpin Creek Formation. Rocks of this member are well exposed along the bluffs of the Potomac River near Balls Bluff Regional Park. The fluvial and deltaic sandstone and siltstone member of the Balls Bluff Siltstone has yielded bones and teeth of a parasuchian (phytosaur) called *Rutiodon* cf. *R. manhattanensis* (Weems, 1979) and a scale of a large coelacanth fish (probably *Diplurus*) (Weems and Kimmel, 1993) from the vicinity of Dulles Airport.

Lacustrine Shale and Siltstone Member

The lacustrine shale and siltstone member (informal) (TRbsh) is predominantly thin-bedded silty and sandy shale interbedded with clayey and sandy siltstone in cyclic sequences as much as 30 ft thick. The unit is gradational with the underlying fluvial sandstone and siltstone member and is considered to be a lateral equivalent. These rocks are also conformably overlain by rocks of the Catharpin Creek Formation. The lacustrine shale beds are poorly exposed but are mapped continuously on the basis of float chips and soil. Arthropod and fish remains, and reptile footprints have been reported from the Manassas Battlefield National Park in Prince William County (Gore, 1988). The fish remains are indeterminate taxonomically. The footprints seem referable to footprint genus *Gwyneddichnium* (Weems, 1993), which was probably made by the tanystropheid aquatic lizard *Gwyneddosaurus*. In addition, Olsen (1988) reported remains of the fish *Semionotus* from the Balls Bluff Siltstone. Parasuchian (phytosaur) teeth have been reported from this member at the Culpeper quarry near Stephensburg, Va., in Culpeper County (Weems, 1992), but otherwise bony remains are rare. Footprints are abundant in the Culpeper quarry and include a medium-size carnivorous dinosaur (*Kayentapus minor*), two small carnivorous dinosaurs (*Grallator sillimani*, *Grallator tuberosus*), a primitive sauropod dinosaur (*Agrestipus hottoni*), a small ornithischian dinosaur (*Gregaripus bairdi*), and possibly an early prosauropod dinosaur (*Eubrontes*), as well as footprints of a large aetosaur (Weems, 1987, 1992).

Catharpin Creek Formation

The Catharpin Creek Formation (JTRc) (Lee and Froelich, 1989) consists of cyclic sequences as much as 100 ft thick of interbedded sandstone, siltstone, and conglomerate. The contact with the underlying Balls Bluff Siltstone is gradational and intertonguing, but the contact with the overlying Mount Zion Church Basalt is a sharp disconformity. The Goose Creek Member (JTRcg) (Lee and Froelich, 1989) of the Catharpin Creek Formation is a lenticular conglomerate composed of subrounded pebbles and cobbles of quartzite, greenstone, metasiltstone, gneiss, and vein quartz, derived from rocks of the Blue Ridge anticlinorium. The conglomerate is interbedded with pebbly arkosic sandstone. Lag gravel deposits from in situ weathering of the conglomerate are diagnostic of this unit when poorly exposed. Like the Leesburg Member of the Balls Bluff Siltstone, the Goose Creek Member probably is debris-flow deposits on an alluvial fan; the distinction between the two is the source and composition of clasts. There are excellent exposures of the conglomerate along Goose Creek, west of Evergreen Mills.

Mesozoic Rocks of the Upper Culpeper Group

The upper part of the Culpeper Group includes the Lower Jurassic series of tholeiitic basalt flows and intercalated sedimentary rocks (Lee and Froelich, 1989) and consists of the Mount Zion Church Basalt, the Midland Formation, the Hickory Grove Basalt, the Turkey Run Formation, and the Sander Basalt.

Mount Zion Church Basalt

The Mount Zion Church Basalt (Jmz) (Lee and Froelich, 1989) is a high-titanium, quartz-normative tholeiitic basalt with vesicular and amygdaloidal tops that mark one or two flows. The basalt is poorly exposed and probably paraconformable with the underlying and overlying strata. The source and conduits of the extrusive basalt flows are uncertain.

Midland Formation

The Midland Formation (Jm) (Lee and Froelich, 1989) consists of cyclic sequences of interbedded siltstone, sandstone, shale, and conglomerate. Lenticular variegated cobble and pebble conglomerate and conglomeratic arkosic sandstone (Jmc) are mapped locally. The rocks of the formation are poorly exposed but are considered to be paraconformable with the basalt flows above and below. The lower part of the Midland Formation has yielded remains of the fish *Diplurus longicaudatus*, *Redfieldius gracilis*, *Semionotus* spp., and *Ptycholepis marshi* from the Midland fish beds in Fauquier County (Baer and Martin, 1949; Parrott and Dunkle, 1949; Schaeffer and others, 1975; Schaeffer and McDonald, 1978; Olsen and others, 1982).

Hickory Grove Basalt

The Hickory Grove Basalt (Jhg) (Lee and Froelich, 1989) is a series of two or three flows of high-titanium, high-iron, quartz-normative tholeiitic basalt with local vesicular and amygdaloidal tops of flows. Locally, the flows are separated by sandstone and siltstone strata (Jhgs) that are locally disconformable but regionally paraconformable with the underlying Midland Formation and the overlying Turkey Run Formation. The unit is poorly exposed but can be seen on the southern side of Goose Creek near Oatlands.

Turkey Run Formation

The Turkey Run Formation (Jtr) (Lee and Froelich, 1989) consists of cyclic sequences of interbedded sandstone, siltstone, conglomerate, and shale. Conglomerate (Jtrc) composed of subrounded boulders, cobbles, and pebbles of greenstone, quartzite, marble, quartz, and basalt is mapped near the border fault. The unit is poorly exposed but can be seen along Little River at Oak Hill, where it has yielded footprints of a small carnivorous dinosaur (*Grallator tenuis*), large prosauropod dinosaurs (*Eubrontes giganteus* and *Eubrontes minusculus*), and an early true crocodile (*Batrachopus*) (Gilmore, 1924; Roberts, 1928; Pannel, 1985; Weems, 1992, 1993).

Sander Basalt

The Sander Basalt (Js) (Lee and Froelich, 1989) is the uppermost sequence of basalt flows in the Culpeper basin. The stratigraphically lower flows are high-titanium, high-iron, quartz-normative basalt that are separated by poorly exposed sandstone and siltstone (Jss) from the stratigraphically higher flows of low-titanium, quartz-normative basalt. The Sander Basalt has distinctive curved columnar joints. The poorly exposed, often saprolitized, basalt is apparently paraconformable with the underlying Turkey Run Formation strata as well as the intercalated sedimentary rocks. This unit can be seen along Little River, east of Aldie.

Thermally Metamorphosed Rocks

The Upper Triassic and Lower Jurassic strata (J̅Rtm) are thermally metamorphosed in zoned contact aureoles adjacent to diabase intrusions throughout the Culpeper basin. Siltstone and shale are altered to cordierite-spotted hornfels in the inner aureole, and epidote-chlorite hornfels characterizes the outer aureole. Sandstones are metamorphosed to tourmaline granofels and (or) quartzite, and carbonate conglomerate is metamorphosed to marble. The largest contact aureoles are found adjacent to the diabase sheets, whereas the contact aureoles adjacent to the dikes are relatively thin.

Diabase Dikes and Sheets

Massive diabase of at least three magma types is recognized in the Culpeper basin (Froelich and Gottfried, 1988) and the adjacent Blue Ridge. (1) Olivine-normative tholeiitic diabase dikes (Jdo) intrude the rocks of the Blue Ridge anticlinorium. (2) Low-titanium, quartz-normative tholeiitic diabase dikes (Jdl) intrude rocks of the Culpeper basin and the Blue Ridge anticlinorium. The long, north-trending diabase dike that intrudes the center of the Culpeper basin is part of a swarm that can be traced into Pennsylvania. (3) High-titanium, quartz-normative tholeiitic diabase (Jdh) occurs as both narrow dikes and thick, differentiated sheets that contain cumulates (Jdc) in the lower parts and late-stage differentiates (Jdg) in the higher parts. The differentiates include granophyre (Jdg), ferrogabbro, diorite, syenite, and aplite. Where chemical or petrographic data are lacking, the diabase composition is not determined, and they are mapped as Jd. The diabase sheets and associated thermal metamorphic aureoles are irregular in shape. The diabase dikes are linear, discontinuous, and en echelon as they were emplaced along fracture systems. The diabase dike exposed along the Potomac River at the northwestern end of Short Hill Mountain has an $^{40}Ar/^{39}Ar$ age of 200 Ma (table 3, sample no. 2). Granophyre and diabase from sheets immediately south of Loudoun County have $^{40}Ar/^{39}Ar$ ages of 200.3±1.2 and 201.2±1.3 Ma, respectively (Sutter, 1988). These dated rocks are herein considered to be emplaced in the Jurassic. Their ages are very near the Triassic-Jurassic boundary that has variously been defined in recent years as occurring from 206 to 199 Ma.

Mesozoic Structure

The Culpeper basin is a half graben that is bounded on the west by an east-dipping normal fault known as the Bull Run fault (Roberts, 1923). The east side of the basin unconformably overlies rocks of the Potomac terrane, but minor normal faults are common. As a consequence of this geometry the strata within the basin generally dip gently west, and the greatest thickness of preserved basin fill is in the western part of the basin. The basin deepened as a result of normal fault movement (Bull Run fault and possible related faults) during the early Mesozoic rifting event that produced similar basins all along the eastern margin of North America.

Folds

The west-dipping, generally homoclinal structure of the Culpeper basin is modified by broad warps with axes at high angles to the border fault, which produce a spread in poles to bedding (fig. 3*N*, on map sheet). Higher amplitude folds with a similar orientation in the Newark basin, known as transverse folds, are considered by Schlische (1992) to have formed as the result of along-strike variation in border-fault displacement. North of Leesburg, the Morven syncline has an axis that parallels the Bull Run fault (Burton and others, 1995). Folds of this type probably result from bedding drag during dip slip movement along the adjacent border fault, which produces local reversals of dip.

Faults

The Bull Run fault is a large normal fault that defines the western edge of the Culpeper basin. For most of its length in Loudoun County the surface trace of the fault is parallel to the Weverton Formation along the east limb of the Blue Ridge anticlinorium. Excavation and well data and rare surface exposures suggest that the fault dips about 45° to 50° (Roberts, 1923; Burton and others, 1995). The minimum displacement along the fault is equal to the greatest thickness of basin sediments, or about 5 mi. Because all units are truncated within the basin, movement along the fault postdates the deposition of strata. Conglomerates within the Culpeper basin suggest erosion of a nearby fault scarp, but the Bull Run fault was not necessarily the only active fault during basin formation, and other synsedimentary Mesozoic faults may lie unrecognized within the Blue Ridge anticlinorium.

Other faults occur within and adjacent to the basin both subparallel and transverse to the strike of basin strata. Transverse faulting is most common in the younger (Jurassic) part of the section; some of these faults offset the border fault and are late structures. Farther east in the basin the map pattern indicates that intrabasin faulting occurred both before and after diabase intrusion. An antithetic, west-dipping normal fault cuts the unconformable basin boundary in the extreme eastern corner of the county. North of Leesburg some northeast-trending cross-basin normal faults are inferred on the basis of stratigraphic models (Burton and others, 1995). These faults are not exposed in Loudoun County but have been traced northward into Maryland (Southworth, 1998). A northwest-trending normal fault truncates these faults and controls the drainage pattern of the Potomac River.

Mesozoic normal faults also have been mapped along the east limb of the Blue Ridge anticlinorium (Burton and others, 1995). The Furnace Mountain fault, east of Catoctin Mountain and just south of the Potomac River, displaces cover-sequence metasedimentary rocks and has a throw of about 328 ft along its northeast-trending leg; it changes direction southward and appears to connect with a northwest-trending cross-basin fault across the Bull Run fault, where there is a small graben. To the south two small downdropped blocks of the Antietam Quartzite within the Harpers Formation occur at or near the intersection of the Bull Run fault with cross-basin normal faults. Whereas Paleozoic shear zones in the Blue Ridge anticlinorium contain extensive greenschist-facies recrystallization and well-developed mylonitic fabric, Mesozoic faulting is characterized by zones of brecciation, cataclasis, and vein-filling mineralization of quartz, calcite, and hematite.

Cenozoic Surficial Deposits

Terraces

High- and low-level terrace deposits of the ancestral Potomac River are preserved on Triassic strata of the Culpeper basin. The conspicuous deposits are composed largely of rounded sandstone and quartzite with *Skolithus* (trace fossil) whose source is west of Loudoun County. The deposits are isolated remnants of former more extensive terraces. Some of the highest deposits in this region, such as Mt. Sterling and east of Lucketts, are probably the result of topographic inversion of an incised channel. The terraced nature of these deposits is best seen from Mt. Sterling to Algonkian Regional Park in the eastern part of the county. These deposits are undated but diabase cobbles are so weathered that they can be cut with a knife.

Lag Gravel

Lag gravel deposits from in situ weathering of conglomerates of the Turkey Run Formation are recognized locally in the western part of the Culpeper basin. Natural exposures superficially resemble terrace deposits but the size and lithology of the clasts are quite different. Excavations near Gleedsville reveal deep deposits of saprolitized cobbles and boulders of quartzite, greenstone, and quartz.

Colluvium

Cobbles, boulders, and blocks of predominantly quartzite and epidosite are concentrated in hillslope depressions by gravity, debris-flow, and freeze-thaw processes. In the Blue Ridge anticlinorium, only large boulder streams, boulder fields, and rock slides are shown on the map because a thin veneer covers virtually all of the mountain slopes (Jacobson and others, 1990; Southworth, 1990). Good examples of boulder streams can be seen near the springs west of the Round Hill Reservoir (McDowell and Milton, 1992). A classic rock slide can be seen on Short Hill Mountain, south of Britain (Southworth, 1995). Boulders of quartzite as much as 3 ft in diameter are well rounded, and elongated blocks of quartzite over 4 ft long are oriented vertically, suggesting the influence of a colder, periglacial climate. Lensoid aprons of subangular clasts of quartzite, phyllite, greenstone, epidosite, and vein quartz cover the strata of the western part of the Culpeper basin and were derived from the escarpment of the east limb of the Blue Ridge anticlinorium; these deposits can be seen along Route 15 north of Lucketts (Burton and others, 1995).

Alluvium

Well to poorly stratified mixtures of clay, silt, sand, gravel, and cobbles underlie flood plains of all tributaries. The channel of the tributary is often on bedrock with alluvium exposed along the banks. Thickness of alluvium is highly variable as a function of bedrock, topography, and land-use practices. Thick alluvium in the Blue Ridge anticlinorium, for example, is related to mill dams and siltation associated with agricultural erosion in the 19th century.

Aeromagnetic Survey

Introduction

An unusually detailed aeromagnetic survey was flown by the U.S. Geological Survey over part of Loudoun County in 1989 to support ongoing geologic mapping. The survey, which covers the Lincoln and most of the Bluemont 7.5-min quadrangles, was flown 500 ft above ground along east-west flightlines spaced 1/8 of a mile apart. High-precision navigational equipment was used (radar ranging system) to provide the positional control that was needed for closely spaced flightlines. The proton magnetometer in the aircraft, which was mounted on a wing tip, sampled the magnetic field every 0.5 sec. Three widely distributed proton magnetometers on the ground recorded the magnetic field at intervals of 2, 6, and 18 sec. These measurements were used to monitor rapid changes in Earth's external magnetic field and to provide the diurnal and possible magnetic storm corrections.

Data Reduction

The aerial magnetometer and navigation measurements were recorded during flight on magnetic tape. These data were reduced by R.E. Bracken to geographic coordinates and corrected magnetic intensity. The resulting point measurements were converted to a Transverse Mercator projection and were gridded at a 75-m interval by using a minimum curvature algorithm (Webring, 1981). The Definitive International Geomagnetic Reference Field (Peddie, 1982) was calculated for the location, altitude, and time of the survey and subtracted from the gridded magnetic data.

The Color-Shaded-Relief Map

This residual magnetic field grid was then processed by a series of programs (Phillips and others, 1993) designed to produce a color-shaded-relief map (fig. 5, on map sheet). The synthetically produced illumination is from the east at a simulated sun angle of 45°. Shadows therefore appear along the western sides of the magnetic anomalies. The relative magnetic intensities of the anomalies are displayed as spectral colors; red corresponds to the higher values. The shading technique greatly enhances small-amplitude magnetic anomalies that are abundant within the central part of the survey. These anomalies normally would be invisible on such commonly used displays, as contour, gray-scale, and color-sliced maps. An overlay of selected geologic contacts from the geologic map provides a framework for relating magnetic anomalies to geologic units.

Correlation of Aeromagnetic Anomalies with Geology

The aeromagnetic anomalies correlate closely with mapped geology because some lithologic units have contrasting magnetic properties. The dominant feature of the magnetic map is a series of large-amplitude magnetic anomalies in three parallel belts associated with the Catoctin Formation (Zc). The western belt that underlies Blue Ridge was only partly sampled by the aeromagnetic survey because the flightlines were terminated on the west over the slopes of the steep mountain front. Magnetic anomalies are associated only with the westernmost (upper) part of the formation and not with the stratigraphically lowest part of the unit on Blue Ridge. The Catoctin Formation along Black Oak Ridge shows strong correlation with moderate-amplitude magnetic anomalies. The broad belt of Catoctin Formation on the east limb of the Blue Ridge anticlinorium is associated with a complex pattern of segmented magnetic highs, some of which are parallel to the strike of the belt and some of which crosscut the strike in a northwest trend. A narrow part of the lowest part of the section appears to be relatively nonmagnetic. Although not recognized in the field, individual basalt flows or groups of flows may be identified by the magnetic anomalies. The origin of the crosscutting anomalies is unknown but may indicate intrusions, such as dikes or faults.

No magnetic anomalies are clearly associated with the Late Proterozoic metadiabase dikes (Zmd) that cut the gneissic core of the Blue Ridge anticlinorium. This lack of correspondence suggests that very little magnetite is present in the dikes. Unpublished field measurements indicate that none of these dikes has a significant magnetic susceptibility. Secondary metamorphic magnetite may have affected the volcanic flows but not the dikes.

All other magnetic anomalies shown in figure 5 have very small amplitudes and are associated either with the basement gneisses or with the overlying metasedimentary rocks of the Fauquier Formation. Two magnetic anomaly trends are evident within this terrane: a northeasterly trend east of the Short Hill fault, which is parallel to the Catoctin trends, and a predominantly northwesterly trend west of the Short Hill fault. Both trends roughly correspond to mapped geologic contacts. Some individually mapped geologic units, such as the graphite-bearing, garnet-rich paragneiss (Yp) and charnockite (Yc) correspond to small-amplitude magnetic anomalies. The anomalies suggest that the units are more continuous and extensive than seen by geologic mapping. Anomalies within the fairly broad area of layered granite gneiss (Ylg) suggest lithologic variations that remain unidentified.

References Cited

Aleinikoff, J.N., Walter, Marianne, Lyttle, P.T., Burton, W.C., Leo, G.W., Nelson, A.E., Schindler, J.S., and Southworth, C.S., 1993, U-Pb zircon and monazite ages of Middle Proterozoic rocks, northern Blue Ridge, Virginia [abs.]: Geological Society of America Abstracts with Programs, v. 25, no. 2, p. 2.

Aleinikoff, J.N., Zartman, R.E., Walter, Marianne, Rankin, D.W., Lyttle, P.T., and Burton, W.C., 1995, U-Pb ages of metarhyolites of the Catoctin and Mount Rogers Formations, central and southern Appalachians; Evidence for two pulses of Iapetan rifting: American Journal of Science, v. 295, no. 4, p. 428–454.

Aleinikoff, J.N., Burton, W.C., Lyttle, P.T., Nelson, A.E., and Southworth, C.S., 2000, U-Pb geochronology of zircon and monazite from Mesoproterozoic granitic gneisses of the northern Blue Ridge, Virginia and Maryland: Precambrian Research, v. 99, nos. 1–2, p. 113–146.

Badger, R.L., and Sinha, A.K., 1988, Age and Sr isotopic signature of the Catoctin volcanic province—Implications for subcrustal mantle evolution: Geology, v. 16, no. 8, p. 692–695.

Baer, F.M., and Martin, W.H., 1949, Some new finds of fossil ganoids in the Virginia Triassic: Science, v. 110, no. 2,869, p. 684–686.

Barker, Fred, and Arth, J.G., 1976, Generation of trondhjemitic-tonalitic liquids and Archean bimodal trondhjemite-basalt suites: Geology, v. 4, no. 10, p. 596–600.

Bassler, R.S., 1919, Cambrian and Ordovician deposits of Maryland: Baltimore, Maryland Geological Survey, 424 p.

Bernknopf, R.L., Brookshire, D.S., Soller, D.R., McKee, M.J., Sutter, J.F., Matti, J.C., and Campbell, R.H., 1993, Societal value of geologic maps: U.S. Geological Survey Circular 1111, 53 p.

Brezinski, D.K., 1992, Lithostratigraphy of the western Blue Ridge cover rocks in Maryland: Maryland Geological Survey Report of Investigations 55, 69 p. and 1:62,500-scale map.

Burton, W.C., and Southworth, C.S., 1993, Garnet-graphite paragneiss and other country rocks in granitic Grenvillian basement, Blue Ridge anticlinorium, northern Virginia and Maryland [abs.]: Geological Society of America Abstracts with Programs, v. 25, no. 4, p. 6.

Burton, W.C., and Southworth, Scott, 2004, Tectonic evolution of the northern Blue Ridge massif, Virginia and Maryland, *in* Tollo, R.P., Corriveau, Louise, McLelland, J.M., and Bartholomew, M.J., eds., Proterozoic tectonic evolution of the Grenville orogen in North America: Geological Society of America Memoir 197, p. 477–493.

Burton, W.C., Froelich, A.J., Schindler, J.S., and Southworth, Scott, 1992a, Geologic map of Loudoun County, Virginia: U.S. Geological Survey Open-File Report 92–716, 17 p. and 1:100,000-scale map.

Burton, W.C., Kunk, M.J., and Lyttle, P.T., 1992b, Age constraints on the timing of regional cleavage formation in the Blue Ridge anticlinorium, northernmost Virginia [abs.]: Geological Society of America Abstracts with Programs, v. 24, no. 2, p. 5.

Burton, W.C., Aleinikoff, J.N., Southworth, C.S., and Lyttle, P.T., 1994, Grenvillian history of intrusion and deformation, northern Blue Ridge, Virginia [abs.]: Geological Society of America Abstracts with Programs, v. 26, no. 4, p. 5–6.

Burton, W.C., Froelich, A.J., Pomeroy, J.S., and Lee, K.Y., 1995, Geology of the Waterford quadrangle, Virginia and Maryland, and the Virginia part of the Point of Rocks quadrangle: U.S. Geological Survey Bulletin 2095, 30 p., 1 pl. in pocket, scale 1:24,000.

Cloos, Ernst, 1951, Structural geology of Washington County, *in* The physical features of Washington County: Baltimore, Maryland Department of Geology, Mines, and Water Resources, p. 124–163.

Drake, A.A., Jr., and Froelich, A.J., 1986, Geologic map of the Fairfax quadrangle, Fairfax County, Virginia: U.S. Geological Survey Geologic Quadrangle Map GQ–1600, scale 1:24,000.

Drake, A.A., Jr., and Lee, K.Y., 1989, Geologic map of the Vienna quadrangle, Fairfax County, Virginia, and Montgomery County, Maryland: U.S. Geological Survey Geologic Quadrangle Map GQ–1670, scale 1:24,000.

Drake, A.A., Jr., and Morgan, B.A., 1981, The Piney Branch Complex—A metamorphosed fragment of the central Appalachian ophiolite in northern Virginia: American Journal of Science, v. 281, no. 4, p. 484–508.

Drake, A.A., Jr., Sinha, A.K., Laird, Jo, and Guy, R.E., 1989, The Taconic orogen, *in* Hatcher, R.D., Jr., Thomas, W.A., and Viele, G.W., eds., The Appalachian-Ouachita orogen in the United States, v. F–2 *of* The geology of North America: Boulder, Colo., Geological Society of America, p. 101–177.

Edwards, Jonathan, Jr., 1988, Geologic map of the Woodsboro quadrangle, Carroll and Frederick Counties, Maryland: Baltimore, Maryland Geological Survey, scale 1:24,000.

Eggleton, R.E., 1975, Preliminary geologic map of the Herndon quadrangle, Virginia: U.S. Geological Survey Open-File Report 75–386, 8 p. and 1:24,000-scale map.

Espenshade, G.H., 1983, Geologic map of a part of the Rectortown quadrangle, Fauquier and Loudoun Counties, Virginia: U.S. Geological Survey Open-File Report 83–503, 5 p. and 1:24,000-scale map.

Espenshade, G.H., 1986, Geology of the Marshall quadrangle, Fauquier County, Virginia: U.S. Geological Survey Bulletin 1560, 60 p.

Evans, N.H., 1991, Latest Precambrian to Ordovician metamorphism in the Virginia Blue Ridge; Origin of the contrasting Lovingston and Pedlar basement terranes: American Journal of Science, v. 291, no. 5, p. 425–452.

Fauth, J.L., and Brezinski, D.K., 1994, Geologic map of the Middletown quadrangle, Frederick and Washington Counties, Maryland: Baltimore, Maryland Geological Survey, scale 1:24,000.

Froelich, A.J., and Gottfried, David, 1988, An overview of early Mesozoic intrusive rocks in the Culpeper basin, Virginia and Maryland, *in* Froelich, A.J., and Robinson, G.R., Jr., eds., Studies of the early Mesozoic basins of the Eastern United States: U.S. Geological Survey Bulletin 1776, p. 151–165.

Froelich, A.J., and Olsen, P.E., 1984, Newark Supergroup, a revision of the Newark Group in eastern North America: U.S. Geological Survey Bulletin 1537–A, p. A55–A58.

Furcron, A.S., 1939, Geology and mineral resources of the Warrenton quadrangle, Virginia: Virginia Geological Survey Bulletin 54, 94 p.

Gathright, T.M., II, and Nystrom, P.G., Jr., 1974, Geology of the Ashby Gap quadrangle, Virginia: Virginia Division of Mineral Resources Report of Investigations 36, 55 p.

Gilmore, C.W., 1924, Collecting fossil footprints in Virginia: Smithsonian Miscellaneous Collections, v. 76, no. 10, p. 16–18.

Gore, P.J.W., 1988, Late Triassic and Early Jurassic lacustrine sedimentation in the Culpeper basin, Virginia, *in* Manspeizer, Warren, ed., Triassic-Jurassic rifting; Continental breakup and the origin of the Atlantic Ocean and passive margins: (New York, Elsevier) Developments in Geotectonics 22, pt. A, p. 369–400.

Herz, Norman, and Force, E.R., 1984, Rock suites in Grenvillian terrane of the Roseland district, Virginia, Part 1, Lithologic relations, *in* Bartholomew, M.J., ed., The Grenville event in the Appalachians and related topics: Geological Society of America Special Paper 194, p. 187–200.

Hillhouse, D.N., 1960, Geology of the Piney River-Roseland titanium area, Nelson and Amherst Counties, Virginia: Blacksburg, Virginia Polytechnic Institute and State University, Ph.D. dissertation, 129 p.

Holden, R.J., 1907, Iron, *in* Watson, T.L., ed., Mineral resources of Virginia: Lynchburg, Va., J.P. Bell Co., p. 402–491.

Horton, J.W., Jr., Drake, A.A., Jr., and Rankin, D.W., 1989, Tectonostratigraphic terranes and their Paleozoic boundaries in the central and southern Appalachians, *in* Dallmeyer, R.D., ed., Terranes in the Circum-Atlantic Paleozoic orogens: Geological Society of America Special Paper 230, p. 213–245.

Irvine, T.N., and Baragar, W.R.A., 1971, A guide to the chemical classification of the common volcanic rocks: Canadian Journal of Earth Sciences, v. 8, no. 5, p. 523–548.

Jacobson, R.B., McDowell, R.C., Milton, D.J., Newell, W.L., Pomeroy, J.S., Schindler, J.S., and Southworth, C.S., 1990, Reconnaissance surficial geologic map of the mountainous parts of Loudoun County, Virginia: U.S. Geological Survey Open-File Report 90–205, 16 oversize sheets, scale 1:12,000.

Jonas, A.I., ed., 1928, Geologic map of Virginia: Charlottesville, Virginia Division of Mineral Resources, scale 1:500,000.

Jonas, A.I., and Stose, G.W., 1938, Geologic map of Frederick County and adjacent parts of Washington and Carroll Counties: Baltimore, Maryland Geological Survey, scale 1:62,500.

Kasselas, G.D., 1993, Stratigraphic framework, structural evolution and tectonic implications of the eastern Blue Ridge sequence in the central Appalachians near Warrenton, Virginia: Blacksburg, Virginia Polytechnic Institute and State University, M.S. thesis, 100 p.

Keith, Arthur, 1894, Description of the Harpers Ferry quadrangle [Va.-Md.-W. Va.]: U.S. Geological Survey Geologic Atlas, Folio 10, 5 p., 4 map sheets, scale 1:125,000.

King, P.B., 1950, Geology of the Elkton area, Virginia: U.S. Geological Survey Professional Paper 230, 82 p.

Kline, S.W., Lyttle, P.T., and Froelich, A.J., 1990, Geologic map of the Loudoun County portion of the Middleburg quadrangle, Virginia: U.S. Geological Survey Open-File Report 90–641, 18 p. and 1:24,000-scale map.

Kline, S.W., Lyttle, P.T., and Schindler, J.S., 1991, Late Proterozoic sedimentation and tectonics in northern Virginia, *in* Schultz, Art, and Compton-Gooding, Ellen, eds., Geologic evolution of the Eastern United States: Virginia Museum of Natural History Guidebook no. 2, p. 263–294.

Kline, S.W., Hertzog, M.G., Lupo, V.E., Swinsky, E.M., Kunk, M.J., and Fleisher, C.J., 1994, Grenville-age ultramafic plutons in the northern Virginia Blue Ridge: Virginia Minerals, v. 40, no. 3/4, p. 17–28.

Kunk, M.J., Froelich, A.J., and Gottfried, D., 1992, Timing of emplacement of diabase dikes and sheets in the Culpeper basin and vicinity, Virginia and Maryland; $^{40}Ar/^{39}Ar$ age spectrum results from hornblende and K-feldspar in granophyres [abs.]: Geological Society of America Abstracts with Programs, v. 24, no. 1, p. 25.

Kunk, M.J., Lyttle, P.T., Schindler, J.S., and Burton, W.C., 1993, Constraints on the thermal history of the Blue Ridge in northernmost Virginia; $^{40}Ar/^{39}Ar$ age dating results [abs.]: Geological Society of America Abstracts with Programs, v. 25, no. 2, p. 31.

Lee, K.Y., 1977, Triassic stratigraphy in the northern part of the Culpeper basin, Virginia and Maryland: U.S. Geological Survey Bulletin 1422–C, 17 p.

Lee, K.Y., 1978, Geologic map of the Arcola quadrangle, Loudoun and Fairfax Counties, Virginia: U.S. Geological Survey Miscellaneous Field Studies Map MF–973, scale 1:24,000.

Lee, K.Y., 1979, Triassic-Jurassic geology of the northern part of the Culpeper basin, Virginia and Maryland: U.S. Geological Survey Open-File Report 79–1557, 19 p., 16 sheets, scale 1:24,000.

Lee, K.Y., 1980, Triassic-Jurassic geology of the southern part of the Culpeper basin and the Barboursville basin, Virginia: U.S. Geological Survey Open-File Report 80–468, 19 p., 18 oversize sheets, scale 1:24,000.

Lee, K.Y., and Froelich, A.J., 1989, Triassic-Jurassic stratigraphy of the Culpeper and Barboursville basins, Virginia and Maryland: U.S. Geological Survey Professional Paper 1472, 52 p.

Leo, G.W., 1990, Geologic map of the northern part of the Rectortown quadrangle, Virginia: U.S. Geological Survey Open-File Report 90–639, 3 p. and 1:24,000-scale map.

McDowell, R.C., and Milton, D.J., 1992, Geologic map of the Round Hill quadrangle, Virginia and West Virginia: U.S. Geological Survey Geologic Quadrangle Map GQ–1702, scale 1:24,000.

Mitra, Gautam, and Elliott, David, 1980, Deformation of basement in the Blue Ridge and the development of the South Mountain cleavage, *in* Wones, D.R., ed., Proceedings of the Caledonides in the USA, International Geological Correlation Programme, Project 27, Caledonide orogen: Blacksburg, Virginia Polytechnic Institute and State University, Department of Geological Sciences Memoir 2, p. 307–311.

Nickelsen, R.P., 1956, Geology of the Blue Ridge near Harpers Ferry, West Virginia: Geological Society of America Bulletin, v. 67, no. 3, p. 239–269.

O'Connor, J.T., 1965, A classification for quartz-rich igneous rocks based on feldspar ratios: U.S. Geological Survey Professional Paper 525–B, p. B79–B84.

Olsen, P.E., 1988, Paleontology and paleoecology of the Newark Supergroup (early Mesozoic, eastern North America), *in* Manspeizer, Warren, ed., Triassic-Jurassic rifting; Continental breakup and the origin of the Atlantic Ocean and passive margins: (New York, Elsevier) Developments in Geotectonics 22, pt. A, p. 185–230.

Olsen, P.E., McCune, A.R., and Thomson, K.S., 1982, Correlation of the early Mesozoic Newark Supergroup by vertebrates, principally fishes: American Journal of Science, v. 282, no. 1, p. 1–44.

Pannel, N.K., 1985, Dinosaur footprints at Oak Hill, Virginia: Washington, D.C., The George Washington University, M.S. thesis, 45 p.

Parker, P.E., 1968, Geologic investigation of the Lincoln and Bluemont quadrangles, Virginia: Virginia Division of Mineral Resources Report of Investigations 14, 23 p., 1 pl. in pocket, scale 1:31,680.

Parrott, W.T., and Dunkle, D.H., 1949, A new occurrence of vertebrate fossils in the Triassic of Virginia [abs.]: Proceedings of the Virginia Academy of Science, 1948–1949, p. 135.

Peddie, N.W., 1982, International Geomagnetic Reference Field—The third generation: Journal of Geomagnetism and Geoelectricity, v. 34, p. 309–326.

Phillips, J.D., Duval, J.S., and Ambroziak, R.A., 1993, National geophysical data grids; Gamma-ray, gravity, magnetic, and topographic data for the conterminous United States: U.S. Geological Survey Digital Data Series DDS–9, one CD-ROM.

Puffer, J.H., and Volkert, R.A., 1991, Generation of trondhjemite from partial melting of dacite under granulite facies conditions; An example from the New Jersey Highlands, USA: Precambrian Research, v. 51, nos. 1–4, p. 115–125.

Rader, E.K., and Evans, N.H., eds., 1993, Geologic map of Virginia—Expanded explanation: Charlottesville, Virginia Division of Mineral Resources, 80 p.

Rankin, D.W., 1975, The continental margin of eastern North America in the southern Appalachians; The opening and closing of the proto-Atlantic Ocean: American Journal of Science, v. 275–A, p. 298–336.

Rankin, D.W., Drake, A.A., Jr., Glover, Lynn, III, Goldsmith, Richard, Hull, L.M., Murray, D.P., Ratcliffe, N.M., Read, J.F., Secor, D.T., Jr., and Stanley, R.S., 1989, Pre-orogenic terranes, *in* Hatcher, R.D., Jr., Thomas, W.A., and Viele, G.W., eds., The Appalachian-Ouachita orogen in the United States, v. F–2 *of* The geology of North America: Boulder, Colo., Geological Society of America, p. 7–100.

Reed, J.C., Jr., 1955, Catoctin Formation near Luray, Virginia: Geological Society of America Bulletin, v. 66, no. 7, p. 871–896.

Reed, J.C., Jr., and Morgan, B.A., 1971, Chemical alteration and spilitization of Catoctin greenstones, Shenandoah National Park, Virginia: Journal of Geology, v. 79, p. 526–548.

Reinhardt, Juergen, 1977, Cambrian off-shelf sedimentation, central Appalachians, *in* Cook, H.E., and Enos, Paul, eds., Deep-water carbonate environments: Society of Economic Paleontologists and Mineralogists Special Publication 25, p. 83–112.

Roberts, J.K., 1923, Triassic basins of northern Virginia: Pan American Geologist, v. 39, no. 3, p. 185–200.

Roberts, J.K., 1928, The geology of the Virginia Triassic: Virginia Geological Survey Bulletin 29, 205 p.

Safford, J.M., 1856, A geological reconnaissance of the State of Tennessee: Nashville, Tennessee Geological Survey, 1st Biennial Report, 164 p.

Schaeffer, Bobb, and McDonald, N.G., 1978, Redfieldiid fishes from the Triassic-Liassic Newark Supergroup of eastern North America: Bulletin of the American Museum of Natural History, v. 159, art. 4, p. 131–173.

Schaeffer, Bobb, Dunkle, D.H., and McDonald, N.G., 1975, *Ptycholepis marshi* Newberry, a chondrostean fish from the Newark Group of eastern North America: Fieldiana Geology, v. 33, no. 12, p. 205–233.

Schlische, R.W., 1992, Structural and stratigraphic development of the Newark extensional basin, eastern North America; Evidence for the growth of the basin and its bounding structures: Geological Society of America Bulletin, v. 104, no. 10, p. 1246–1263.

Schwab, F.L., 1986, Latest Precambrian-earliest Paleozoic sedimentation, Appalachian Blue Ridge and adjacent areas—Review and speculation, *in* McDowell, R.C., and Glover, Lynn, III, eds., Studies in Appalachian geology (Lowry volume): Blacksburg, Virginia Polytechnic Institute and State University, Department of Geological Sciences Memoir 3, p. 115–137.

Sinha, A.K., and Bartholomew, M.J., 1984, Evolution of the Grenville terrane in the central Virginia Appalachians, *in* Bartholomew, M.J., ed., The Grenville event in the Appalachians and related topics: Geological Society of America Special Paper 194, p. 175–186.

Smoot, J.P., 1989, Fluvial and lacustrine facies of the early Mesozoic Culpeper basin, Virginia and Maryland, July 14, 1989: Field Trip Guidebook T213 for the 28th International Geological Congress: Washington, D.C., American Geophysical Union, 15 p.

Southworth, C.S., 1990, Hydrogeologic setting of springs on Short Hill Mountain, Loudoun County, northern Virginia: U.S. Geological Survey Miscellaneous Field Studies Map MF–2112, scale 1:24,000.

Southworth, C.S., 1991, Geologic map of the Loudoun County, Virginia, part of the Harpers Ferry quadrangle: U.S. Geological Survey Miscellaneous Field Studies Map MF–2173, 12 p. and 1:24,000-scale map.

Southworth, C.S., 1994, Geologic map of the Bluemont quadrangle, Loudoun and Clarke Counties, Virginia: U.S. Geological Survey Geologic Quadrangle Map GQ–1739, scale 1:24,000.

Southworth, C.S., 1995, Geologic map of the Purcellville quadrangle, Loudoun County, Virginia: U.S. Geological Survey Geologic Quadrangle Map GQ–1755, scale 1:24,000.

Southworth, C.S., 1998, Geologic map of the Poolesville quadrangle, Frederick and Montgomery Counties, Maryland and Loudoun County, Virginia: U.S. Geological Survey Geologic Quadrangle Map GQ–1761, 12 p. and 1:24,000-scale map.

Southworth, Scott, 2005, Kinematics of the Short Hill fault; Late Paleozoic contractional reactivation of an early Paleozoic extensional fault, Blue Ridge-South Mountain anticlinorium, northern Virginia and southern Maryland: U.S. Geological Survey eBulletin 2136, 88 p.

Southworth, Scott, and Brezinski, D.K., 1996, Geology of the Harpers Ferry quadrangle, Virginia, Maryland, and West Virginia: U.S. Geological Survey Bulletin 2123, 33 p., 1 pl. in pocket, scale 1:24,000.

Stose, A.J., and Stose, G.W., 1946, Geology of Carroll and Frederick Counties, *in* The physical features of Carroll County and Frederick County: Baltimore, Maryland Department of Geology, Mines, and Water Resources, p. 11–131.

Stose, G.W., 1906, The sedimentary rocks of South Mountain, Pennsylvania: Journal of Geology, v. 14, p. 201–220.

Streckeisen, A., 1976, To each plutonic rock its proper name: Earth-Science Reviews, v. 12, no. 1, p. 1–33.

Sutter, J.F., 1988, Innovative approaches to the dating of igneous events in the early Mesozoic basins of the Eastern United States, *in* Froelich, A.J., and Robinson, G.R., Jr., eds., Studies of the early Mesozoic basins of the Eastern United States: U.S. Geological Survey Bulletin 1776, p. 194–200.

Toewe, E.C., 1966, Geology of the Leesburg quadrangle, Virginia: Virginia Division of Mineral Resources Report of Investigations 11, 52 p., 1 pl. in pocket, scale 1:24,000.

Tollo, R.P., and Aleinikoff, J.N., 1992, The Robertson River Igneous Suite, Virginia Blue Ridge; A case study in multiple-stage magmatism associated with the early stages of Iapetan rifting [abs.]: Geological Society of America Abstracts with Programs, v. 24, no. 2, p. 70.

Tollo, R.P., and Lowe, T.K., 1994, Geologic map of the Robertson River Igneous Suite, Blue Ridge province, northern and central Virginia: U.S. Geological Survey Miscellaneous Field Studies Map MF–2229, scale 1:100,000.

Tollo, R.P., Lowe, T.K., Arav, Sara, and Gray, K.J., 1991, Geology of the Robertson River Igneous Suite, Blue Ridge province, Virginia, *in* Schultz, Art, and Compton-Gooding, Ellen, eds., Geologic evolution of the Eastern United States: Virginia Museum of Natural History Guidebook no. 2, p. 229–262.

Webring, Michael, 1981, MINC; A gridding program based on minimum curvature: U.S. Geological Survey Open-File Report 81–1224, 43 p.

Weems, R.E., 1979, A large parasuchian (phytosaur) from the Upper Triassic portion of the Culpeper basin of Virginia (USA): Proceedings of the Biological Society of Washington, v. 92, no. 4, p. 682–688.

Weems, R.E., 1987, A Late Triassic footprint fauna from the Culpeper basin, northern Virginia (USA): American Philosophical Society Transactions, v. 77, pt. 11, p. 1–79.

Weems, R.E., 1992, A re-evaluation of the taxonomy of Newark Supergroup saurischian dinosaur tracks, using extensive statistical data from a recently exposed tracksite near Culpeper, Virginia, *in* Sweet, Palmer, ed., Proceedings of the 26th Forum on the Geology of Industrial Minerals: Charlottesville, Virginia Division of Mineral Resources Publication 119, p. 113–127.

Weems, R.E., 1993, Stratigraphic distribution and bibliography of fossil fish, amphibians, and reptiles from Virginia: U.S. Geological Survey Open-File Report 93–222, 49 p.

Weems, R.E., and Kimmel, P.G., 1993, Upper Triassic reptile footprints and a coelacanth fish scale from the Culpeper basin, Virginia: Proceedings of the Biological Society of Washington, v. 106, no. 2, p. 390–401.

Wehr, F.L., II, 1985, Stratigraphy of the Lynchburg Group and Swift Run Formation, Late Proterozoic (730–570 Ma), central Virginia: Southeastern Geology, v. 25, no. 4, p. 225–239.

Whitaker, J.C., 1955, Direction of current flow in some Lower Cambrian clastics in Maryland: Geological Society of America Bulletin, v. 66, no. 6, p. 763–766.

Wilson, J.T., 1966, Did the Atlantic close and then re-open?: Nature, v. 211, p. 676–681.